DE SITTER VACUA AND INFLATION IN NO-SCALE SUPERGRAVITY

A Dissertation

by

BALAKRISHNAN NAGARAJ

Submitted to the Graduate and Professional School of
Texas A&M University
in partial fulfillment of the requirements for the degree of

DOCTOR OF PHILOSOPHY

Chair of Committee,	Dimitri Nanopoulos
Committee Members,	Bhaskar Dutta
	Teruki Kamon
	Stephen Fulling
Head of Department,	Grigory Rogachev

August 2022

Major Subject: Physics

ABSTRACT

We construct Lagrangians and show new Minkowski and de Sitter solutions with the presence of multiple chiral fields in a framework of 4d $\mathcal{N} = 1$ no-scale supergravity in a unified way. The framework is chosen as it naturally arises in the low energy limit of string theories. The de Sitter solutions are particularly relevant given that our universe is expanding at an accelerated rate. The mechanics of these constructions are to first solve for Minkowski solutions and then "combine" antipodal Minkowski solutions to obtain a de Sitter solution. Quartic stabilization terms are added to Kähler potential in order to stabilize the de Sitter solutions, and then we proceed to generalize our solutions in the presence of various matter fields. With matter fields, it becomes possible to "perturb" the de Sitter solutions to find inflationary potentials. Hence our constructions give a way of obtaining Minkowski, de Sitter, and inflationary potentials in a unified way.

DEDICATION

To my Mother and Sister.

ACKNOWLEDGMENTS

I am eternally grateful to my advisor Dr. Dimitri Nanopoulos for being a superb mentor and allowing me to pursue my various interests during my Ph.D. He is always a constant source of inspiration, and his physical insights helped me immensely with my research. I also had the privilege to sit in some of his fantastic courses, which later became the foundation of my research.

As part of my research, I was lucky to have worked with Dr. John Ellis and Dr. Keith Olive. They helped me identify deeper structures in physics that were not readily visible. My interactions with them are some of the most cherished moments of my graduate student life.

Special thanks to Dr. Bhaskar Dutta, Dr. Teruki Kamon and Dr. Stephan Fulling for accepting to be part of my dissertation committee. Their comments and inputs at the various stages of my work were extremely valuable.

I am also hugely indebted to Dr. Bhaskar Dutta, who helped me with research assistantships during the crucial part of my Ph.D. I would also like to thank Dr. Marlan Scully, who funded me during the final stages of my Ph.D.

I also thank Dr. Katrin Becker and Dr. Christopher Pope for many simulating discussions inside and outside of the class. Many of the physics that I learned in their classes will always stay with me for the rest of my life.

Special thanks to Dr. Dmitry Ponomarev, who was at Texas A&M University as a post-doctoral researcher for two years. My many discussions with him and the eventual collaboration resulting in some beautiful results are the high points of my graduate research.

I would also like to thank my colleagues Arash Azizi, Sunny Guha, Surya Kiran Kanumilli, Zhijin Li, Tuo Jia, Zhaojie Xu, Aritra Saha, and Anindya Sengupta for all the wonderful discussions during the journal club meetings.

Finally, I would like to thank my parents and my dear sister, without whose constant support and encouragement I would not have been able to finish my Ph.D. successfully.

CONTRIBUTORS AND FUNDING SOURCES

Contributors

This work was reviewed by a dissertation committee consisting of Prof. Dimitri Nanopoulos, Prof. Bhaskar Dutta and Prof. Teruki Kamon of the Department of Physics and Astronomy and Prof. Stephen Fulling of the Department of Mathematics.

Funding Sources

My graduate research was funded by teaching fellowship from Texas A&M University and by Mitchell/Heep Chair in High Energy Physics, Texas A&M University.

NOMENCLATURE

SUGRA	Supergravity
dS	de Sitter
AdS	Anti-de Sitter
KKLT model	Kachru, Kallosh, Linde and Trivedi model
4d	Four dimensional
VEV	Vacuum Expectation Value

TABLE OF CONTENTS

Page

LIST OF FIGURES

FIGURE Page

1. INTRODUCTION AND LITERATURE REVIEW

In recent years interest has grown in the possibility of string solutions in de Sitter space, for at least a couple of practical reasons. One is the discovery of the expansion of the universe in the present time is accelerating due to non-vanishing vacuum energy that is small relative to the energy scale of the Standard Model [1]. The other is the growing observational support for inflationary cosmology [2], according to which the early universe underwent an epoch of near-exponential quasi-de Sitter expansion driven by vacuum energy that was large compared with the energy scale of the Standard Model, but still hierarchically smaller than the Planck scale. All of a sudden it became important to incorporate a small positive cosmological constant into string theory that was being developed as a theory of everything describing all the particles and the forces of nature including gravity. One of the most appealing constructions of a de Sitter vacua (or a vacuum with a positive cosmological constant) is the KKLT model [3]. KKLT start with warped Type IIB compactifications with non-trivial NS and RR fluxes and construct a supersymmetric AdS vacuum. Then anti-D3 branes are put on top of the AdS vacuum to lift it to a metastable dS vacuum. However this construction isn't rigorously proved yet, and is beset with various problems like existence of tachyons in dS, backreaction of anti-D branes and other problems. Another school of thought is that dS solutions cannot exist in string theory. [4] derived phenomenological criteria that put all dS vacua including KKLT construction into the so called swampland. Swampland is suppose to represent the set of solutions that seem innocuous at low energies but suffers from various problems at high energies. It is true that there has not been even a single rigorous dS vacuum construction in string theory, but to put forward such a dramatic statement seems premature. It only seems prudent to sit down and double our efforts toward finding a dS solution within string theory. It may very well be that string theory is the correct theory of quantum gravity but the way it provides a dS vacuum is much more sophisticated than what has been attempted so far [5].

In pursuit of rigorous dS solutions in string theory, we propose to start small by constructing dS vacuum in $\mathcal{N} = 1$ supergravity theories that are low energy effective theories of string theories. It is

our belief that such constructions could be signposts for deriving rigorous dS solutions within string theory itself. Indeed, it has been possible to put constraints on low energy theories based on the criteria that the high energy theory behaves well. So it is very well possible that our supergravity dS solutions are at least not within the swampland. One interesting class of supergravity theories are the no-scale supergravity theories [6, 10]. It has been shown that the no-scale supergravity emerges as the effective field theory resulting from a supersymmetry-preserving compactifications of ten-dimensional supergravity, used as a proxy for compactification of heterotic string theory [11]. This was first shown in the context of a simplified model of compactification with a single volume modulus, but this first example has been extended to multifield models, including compactifications with three complex Kahler moduli and a complex coupling modulus, as well as some number of complex structure moduli. The unique Kahler potential for an $\mathcal{N} = 1$ supergravity model with a single chiral superfield ϕ was found in [6] as

$$K = -3 \ln \left(\phi + \phi^{\dagger} \right) . \tag{1.1}$$

The no-scale models have been named as such because the scale of supersymmetry breaking is undetermined at the tree level and it was suggested that the scale is set by the perturbative corrections to the low-energy effective field theory [7].

Construction of dS vacua (along with Minkowski and AdS vacua) was done in no-scale models with a single chiral field [6]. It seems natural to extend the results to theories with multiple chiral fields. By doing so, we are broadening the set of solutions that might fall outside the swampland. Much of the work in [12], co-authored by the author of this dissertation, is focused towards this goal. Along the way, some valuable results regarding Minkowski vacuum in no-scale models were also obtained in [12]. Some of the concrete results from [12] are as follows:

1. Construction of multifield Minkowski solutions along with special solutions (called kink solutions in [12]) that are flat in both real and imaginary field directions.

2. Construction of dS solutions by combining two (antipodal) superpotentials corresponding to

Minkowski solutions.

3. Stability and holomorphy analysis of both the Minkowski and dS solutions.

Once we have de Sitter solutions further generalizations are possible. In [13], we construct Minkowski and de Sitter solutions in presence of matter fields and then proceed to "perturb" the de Sitter solutions to get inflationary potentials. Some of the concrete results from [13] are as follows:

1. Further generalization of the superpotentials leading to Minkowski and de Sitter solutions.

2. Construction of Minkowski and de Sitter solutions in presence of twisted and untwisted matter fields.

3. Addition of inflationary superpotential term to de Sitter superpotential to get Starobinsky-like inflationary potentials.

The rest of the dissertation is a detailed overview of the above results. In chapter 2 of this dissertation, we discuss de Sitter solutions in single field models and elaborate on the stability of the solution and the conditions for holomorphy of the superpotential. We then extend the single field solution to include multiple fields. As a byproduct, we discover new Minkowski solutions in multi-field no-scale models. We also discuss the stability and holomorphy conditions for multi-field models and give examples whose superpotential contains only integer powers of the chiral fields. In chapter 3, we discuss the uniqueness of single-field monomial superpotentials leading to a Minkowski vacuum and how they can be combined in pairs to yield dS vacua. We also provide another geometrical interpretation of the Minkowski and de Sitter solutions. We then further extend these constructions to include twisted and untwisted matter fields. This is followed by a discussion of inflationary models with either untwisted or twisted matter fields. In chapter 4, we conclude by discussing some possible extensions of work.

2. DE SITTER VACUA IN NO-SCALE SUPERGRAVITY[1]

2.1 Introduction

The unique Kähler potential for 4d $\mathcal{N} = 1$ supergravity model with a single chiral superfield ϕ (up to canonical field redefinitions) was found in [6] to be

$$K \;=\; -3\,\ln\left(\phi+\phi^\dagger\right)\,. \tag{2.1}$$

In [7] this was dubbed 'no-scale supergravity', because the scale of supersymmetry breaking is undetermined at the tree level, and it was suggested that the scale might be set by perturbative corrections to the effective low-energy field theory. The single-field model [6] was explored in more detail in [8], and the generalization to more superfields was developed in [9] [2].

If string theory admits de Sitter solutions and approximate supersymmetry with scales hierarchically smaller than the string scale, their low-energy dynamics should be described by some suitable supergravity theory that is capable of incorporating the breaking of supersymmetry that is intrinsic in de Sitter space. Since string compactifications yield no-scale supergravity as an effective low-energy field theory, it is natural to investigate how de Sitter space could be accommodated within no-scale supergravity [3]. This question was studied already in [8], and the purpose of this chapter is to analyze this question in more detail and generality, extending the previous single-field analysis of [8, 16] to no-scale models with multiple superfields that are characteristic of generic string compactifications. These models may provide a useful guide to the possible forms of effective field theories describing the low-energy dynamics in de Sitter solutions of string theory, assuming that they exist.

The outline of this chapter is as follows. In Section 2.2 we review the original motivation and

[1] Reprinted with permission from "De Sitter Vacua in No-Scale Supergravity" by J. Ellis, B. Nagaraj, D. V. Nanopoulos and K. A. Olive, 2018, Springer Nature, JHEP 1811 (2018) 110. Copyright [2018] by the authors.

[2] For a review of early work on no-scale supergravity, see [10].

[3] For other approaches, see [15].

construction of no-scale supergravity with a vanishing cosmological constant [6], and also review the construction in [8, 16] of no-scale supergravity models with non-vanishing vacuum energy. Section 2.3 describes the extensions of these models to no-scale supergravity models with two chiral fields, which have an interesting geometrical visualization. The de Sitter construction is extended to multiple chiral fields in Section 2.4. In each case, we discuss the requirements of stability of the vacuum and holomorphy of the superpotential, and give examples of models whose superpotentials contain only integer powers of the chiral fields. Finally, Section 2.5 summarizes our conclusions.

2.2 Single-Field Models

2.2.1 No-Scale Supergravity Models

We recall that the geometry of a $N = 1$ supergravity model is characterized by a Kähler potential K that is a Hermitian function of the complex chiral fields ϕ^i. The kinetic terms of these fields are

$$K_i^j \frac{\partial \phi_i}{\partial x_\mu} \frac{\partial \phi_j^\dagger}{\partial x^\mu} \qquad \text{where} \qquad K_i^j \equiv \frac{\partial^2 K}{\partial \phi^i \partial \phi_j^\dagger} \tag{2.2}$$

is the Kähler metric. Defining also $K_i \equiv \partial K / \partial \phi^i$ and analogously its complex conjugate K^i, the tree-level effective potential is

$$V = e^K \left[K^j K_i^{-1j} K_i - 3 \right] + \frac{1}{2} D^a D^a \,, \tag{2.3}$$

where K_i^{-1j} is the inverse of the Kähler metric Eq. (2.2) and $\frac{1}{2} D^a D^a$ is the D-term contribution, which is absent for chiral fields that are gauge singlets as we assume here.

In this Section we consider the case of a single chiral field ϕ, in which case it is easy to verify that the first term in Eq. (2.3) can be written in the form

$$V(\phi) = 9\, e^{4K/3}\, K^{-1}_{\phi\phi^\dagger}\, \partial_\phi \partial_{\phi^\dagger} e^{-K/3} \,. \tag{2.4}$$

It is then clear that the unique form of K with a Minkowski solution, for which $V = 0$, is

$$K \;=\; -3\,\ln\left(f(\phi) + f^\dagger(\phi^\dagger)\right)\,, \tag{2.5}$$

where f is an arbitrary analytic function. In fact, since physical results are unchanged by canonical field transformations, one can transform $f(\phi) \to \phi$ and recover the simple form Eq. (2.1) of the Kähler potential for a no-scale supergravity model with a single chiral field.

We note that this Kähler potential describes a maximally-symmetric SU(1,1)/U(1) manifold whose Kähler curvature $R_i^j \;\equiv\; \partial_i \partial^j \ln K_i^j$ obeys the simple proportionality relation

$$\frac{R_i^j}{K_i^j} \;\equiv\; R \;=\; \frac{2}{3}\,, \tag{2.6}$$

which is characteristic of an Einstein-Kähler manifold.

This model was generalized in EKN [8], where general solutions for all flat potentials were found. The SU(1,1) invariance in Eq. (2.5) holds whenever [4]

$$R \;\equiv\; \frac{R_i^j}{K_i^j} \;=\; \frac{2}{3\alpha}\,, \tag{2.7}$$

which corresponds (up to irrelevant field redefinitions) to the extended Kähler potential

$$G \;=\; K + \ln W(\phi) + \ln W^\dagger(\phi^\dagger)\,, \tag{2.8}$$

where

$$K \;=\; -3\,\alpha \ln(\phi + \phi^\dagger)\,, \tag{2.9}$$

[4] We note that in extended SU(N,1) no-scale models [9] that include $N-1$ matter fields, y_i, with the Kähler potential $K = -3\alpha \log(\phi + \phi^\dagger - y^i y_i^\dagger/3)$, the Kähler curvature becomes $R = (N+1)/3\alpha$. Our constructions can be generalized to this case, but such generalizations lie beyond the scope of this work.

we assume $\alpha > 0$, and $W(\phi)$ is the superpotential [5]. In this case the effective potential is

$$V \;=\; e^{G}\left[G^{j}K_{i}^{-1j}G_{i} - 3\right]\,. \tag{2.10}$$

EKN found three classes of solutions with a constant scalar potential [8], namely

$$1) \qquad W \;=\; a \qquad \text{and} \qquad \alpha = 1\,, \tag{2.11}$$

$$2) \qquad W \;=\; a\,\phi^{3\alpha/2}\,, \tag{2.12}$$

$$3) \qquad W \;=\; a\,\phi^{3\alpha/2}(\phi^{3\sqrt{\alpha}/2} - \phi^{-3\sqrt{\alpha}/2})\,. \tag{2.13}$$

Solution 1) corresponds to the $V = 0$ Minkowski solution discussed above, whereas solutions 2) and 3) yield potentials that are constant in the real direction, but are in unstable in the imaginary direction. As we discuss further below, stabilization in the imaginary direction is straightforward and allows these solutions to be used for realistic models with constant non-zero potentials in the real direction. We find that 2) leads to anti-de Sitter solutions with $V = -3/8^{\alpha}\cdot a^2$ and 3) leads to de Sitter solutions [6] with $V = 3\cdot 2^{2-3\alpha}\cdot a^2$. We note that in the particular case $\alpha = 1$ this reduces to $W = a\,(\phi^3 - 1)$, which yields the de Sitter solution discussed in [16]. This was utilized in [19] when making the correspondence between no-scale supergravity and R^2 gravity.

In the following subsections, we first generalize the Minkowski solution Eq. (2.11), and then show that de Sitter solutions can be obtained as combinations of Minkowski solutions. These aspects of the solutions will subsequently be used to generalize them to model theories with multiple moduli.

2.2.2 Minkowski Solutions

We consider the $N = 1$ no-scale supergravity model with a single complex chiral field ϕ described by the Kähler potential given in Eq. (2.9) and the superpotential $W(\phi)$ is a monomial of

[5] Starobinsky-like models with $\alpha \neq 1$ were discussed in [17]. Such models were later dubbed α-attractors in [18, 16].

[6] We correct here a typo in the third solution given in [8].

the form

$$W \;=\; a\,\phi^n\,, \tag{2.14}$$

and we seek the value of n that admits a Minkowski solution with $V = 0$. Defining $\phi \equiv x + iy$, the potential along real field direction x is given by

$$V \;=\; 2^{-3\alpha}\cdot\left(\frac{(2n-3\alpha)^2}{3\alpha}-3\right)\cdot a^2\cdot x^{2n-3\alpha}\,. \tag{2.15}$$

We can obtain a Minkowski solution by setting to zero the term in the brackets:

$$\frac{(2n-3\alpha)^2}{3\alpha} \;=\; 3. \tag{2.16}$$

Solving the above equation for n, we find two solutions [16]:

$$n_\pm \;=\; \frac{3}{2}(\alpha \pm \sqrt{\alpha})\,. \tag{2.17}$$

We note that $n_- = 0$ for $\alpha = 1$, corresponding to the EKN solution Eq. (2.11) listed above. However, we see that in addition to this $n = 0$ solution, $n = 3$ also yields a Minkowski solution with $V = 0$ in all directions in field space.

Although such solutions exist for any α, for the superpotential to be holomorphic we need $n_- \geq 0$, which requires $\alpha \geq 1$. Clearly, integer solutions for n are obtained whenever α is a perfect square [16].

It is possible to go from one superpotential to another via a Kähler transformation:

$$K \;\longrightarrow\; K + \lambda(\phi) + \lambda^\dagger(\phi^\dagger), \qquad W \;\longrightarrow\; e^{-\lambda(\phi)}W\,. \tag{2.18}$$

with $\lambda(\phi) \;=\; \pm 3\sqrt{\alpha}\,\ln\phi$. In general, the solutions given in Eq. (2.17) can be thought of as corresponding to endpoints of a line segment of length $3\sqrt{\alpha}$ centred at $3\alpha/2$. Though this appears trivial, extensions of this geometric visualization will be useful in the generalizations to multiple

fields discussed below.

For $\alpha \neq 1$, the two solutions yield $V = 0$ only along the real direction, and the mass squared of the imaginary component y along the real field direction for $x > 0$ and $y = 0$ is given by

$$m_y^2 \;=\; 2^{2-3\alpha} \cdot \frac{(\alpha - 1)}{\alpha} \cdot a^2 \cdot x^{\pm 3\sqrt{\alpha}}, \tag{2.19}$$

where the $\pm$ in the exponent corresponds to the two solutions $n_\pm$. From this it is clear that the Minkowski solutions are stable for $\alpha \geq 1$.

There are two aspects of the single-field model that we emphasize here, because they generalize in an interesting way to multi-field models. The first is the fact that there are two solutions for n and the second is that, when $\alpha = 1$, we get a Minkowski solution with a potential that vanishes everywhere.

2.2.3 De Sitter Solutions

As was shown in EKN, de Sitter solutions can be found with the Kähler potential Eq. (2.9) and a superpotential of the form Eq. (2.13), which may be written as

$$W \;=\; a\,(\phi^{n_-} - \phi^{n_+})\,, \tag{2.20}$$

where $n_\pm$ are given in Eq. (2.17). In this case the potential along the real field direction $y = 0$ is

$$V \;=\; 3 \cdot 2^{2-3\alpha} \cdot a^2\,. \tag{2.21}$$

Thus, the de Sitter solution is obtained by taking the difference of the two “endpoint" solutions mentioned above.

Unfortunately, this de Sitter solution is not stable for finite α. However, this can be remedied by deforming the Kähler potential to the following form [20, 17]:

$$K \;=\; -\,3\,\alpha \ln(\phi + \phi^\dagger + b(\phi - \phi^\dagger)^4) :\; b \;>\; 0\,. \tag{2.22}$$

The addition of the quartic stabilization term does not modify the potential in the real direction, which is still given by Eq. (2.21). However, the squared mass of the imaginary component y is now given by

$$m_y^2 \;=\; \frac{2^{2-3\alpha}}{\alpha}\cdot a^2\cdot x^{-3\sqrt{\alpha}}\cdot\left(\alpha(x^{3\sqrt{\alpha}}-1)^2-(1-96bx^3)(x^{3\sqrt{\alpha}}+1)^2\right)\,. \tag{2.23}$$

The stability requirement $m_y^2 \geq 0$ is achieved when $\alpha \geq 1$. In Fig. 2.1 we plot the stabilized potential for $a = b = \alpha = 1$, and we see that the potential is completely flat along the line $y = 0$ and is stable for all values of $x > 0$.

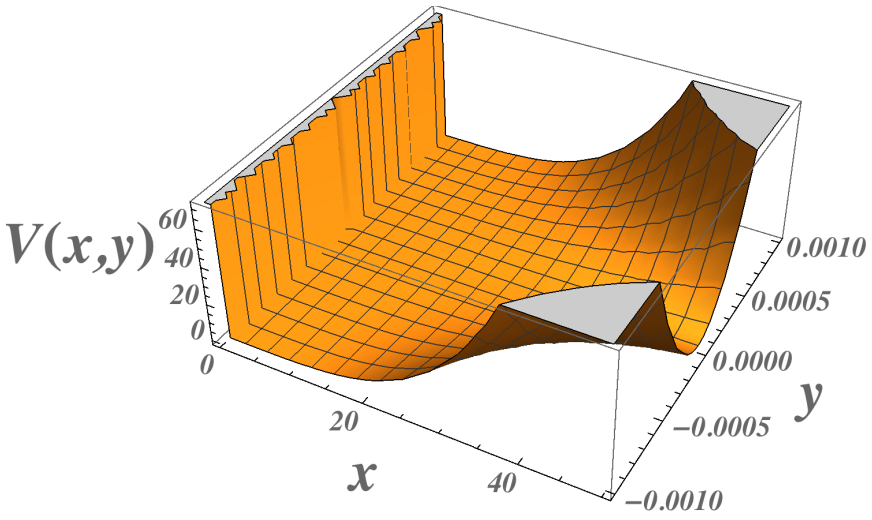

Figure 2.1: The potential $V(x, y)$ for $a = b = \alpha = 1$ in no-scale supergravity with the stabilized Kähler potential Eq. (2.22) and the superpotential Eq. (2.20). Reprinted with permission from [12].

2.3 Two-Field Models

Several of the features of the single-field model that we discussed in Section 2.2 generalize in an interesting geometrical way to models with $N > 1$ fields. We illustrate this first by considering in this section the simplest generalization, i.e., two-field models.

2.3.1 Minkowski Solutions

We consider the following Kähler potential with two complex chiral fields:

$$K \;=\; -3\sum_{i=1}^{2}\alpha_i \ln(\phi_i+\phi_i^\dagger)\,:\;\alpha_i\;>\;0\,. \tag{2.24}$$

with the following ansatz for the superpotential

$$W=\;a\prod_{i=1}^{2}\phi_i^{n_i}\,. \tag{2.25}$$

Denoting the real and imaginary parts by $\phi_i = x_i + iy_i$, we find that the potential along the real field directions $y_i = 0$ is given by

$$V=\;\left(\sum_{i=1}^{2}\frac{(2n_i-3\alpha_i)^2}{3\alpha_i}-3\right)\cdot a^2\cdot\left(\prod_i^2 2^{-3\alpha_i}x_i^{2n_i-3\alpha_i}\right)\,. \tag{2.26}$$

We see immediately that by setting

$$\sum_{i=1}^{2}\frac{(2n_i-3\alpha_i)^2}{3\alpha_i}\;=\;3 \tag{2.27}$$

we obtain a Minkowski solution,

We observe that Eq. (2.27) describes an ellipse in the (n_1, n_2) plane centred at $(3\alpha_1/2, 3\alpha_2/2)$. All choices of (n_1, n_2) lying on this ellipse yield a Minkowski solution. In this way, the line segment centred at $3\alpha/2$ in the single-field model that yielded Minkowski endpoints is generalized, and we obtain a one-dimensional continuum subspace of Minkowski solutions. We can conveniently parametrize the solutions for n_i in Eq. (2.27) as the points on the ellipse corresponding to unit vectors $\vec{r} = (r_1, r_2)$ with $r_1^2 + r_2^2 = 1$:

$$n_{i\pm}\;=\;\frac{3}{2}\left(\alpha_i\pm\frac{r_i}{\sqrt{\sum_{j=1}^{2}\frac{r_j^2}{\alpha_j}}}\right)\,,\qquad i=1,2\,. \tag{2.28}$$

The unit vector $\vec{r}$ should be located starting at the centre of the ellipse, and defines a direction on its circumference. The operation $\vec{r} \to -\vec{r}$ in Eq. (2.28) takes a point on the ellipse to its antipodal point, an observation we use later to construct de Sitter solutions. We note also that holomorphy requires both $n_1, n_2 \geq 0$, i.e.

$$\alpha_i + \frac{r_i}{\sqrt{\sum_{j=1}^{2} \frac{r_j^2}{\alpha_j}}} \;\geq\; 0\,, \qquad i = 1, 2\,. \tag{2.29}$$

As in the case of the single-field model, we can move from one point on the ellipse to another point via a Kähler transformation. This is possible because the superpotential is just a monomial.

Integer solutions for the values of n_i are also possible in the two-field case. The full set of solutions in the single-field case are valid for $n_{1\pm}$ when $n_{2+} = n_{2-}$ (and similarly when $1 \leftrightarrow 2$). More generally, solutions can be found by writing

$$(n_{1+} - n_{1-})^2 \;=\; \lambda_1(n_{1+} + n_{1-}) \qquad \text{and} \qquad (n_{2+} - n_{2-})^2 \;=\; \lambda_2(n_{2+} + n_{2-})\,, \tag{2.30}$$

with λ_i is non-negative and $\lambda_1 + \lambda_2 = 3$. As one example out of an infinite number of solutions, choosing $\lambda_1 = 1$ and $\lambda_2 = 2$ gives $(n_{1+}, n_{1-}) = (3, 1)$ and $(n_{2+}, n_{2-}) = (6, 2)$.

In general, points around the ellipse yield potentials that are flat only in the real direction and, as in the single-field model, may not be stable in the imaginary directions. The masses of the imaginary component fields y_1, y_2 are given by

$$m_{y_i}^2 \;=\; \frac{2^{2-3(\alpha_1+\alpha_2)}}{\alpha_i^2} \cdot \left(\alpha_i^2 - \frac{r_i^2}{\left(\sum_{j=1}^{2} \frac{r_j^2}{\alpha_j} \right)} \right) \cdot a^2 \cdot x_1^{2n_1 - 3\alpha_1} x_2^{2n_2 - 3\alpha_2}\,, \qquad i = 1, 2\,. \tag{2.31}$$

The stability requirement $m_{y_i}^2 \geq 0$ for $x_i > 0$ implies

$$\alpha_i^2 - \frac{r_i^2}{\left(\sum_{j=1}^{2} \frac{r_j^2}{\alpha_j} \right)} \;\geq\; 0\,, \qquad i = 1, 2\,. \tag{2.32}$$

It is easy to see that if the stability conditions are satisfied then the holomorphy conditions Eq. (2.29) are satisfied. Since the left hand side of Eq. (2.32) is proportional to $n_{i+}n_{i-}$, points on the ellipse that give stable Minkowski solution are those that are holomorphic so long as their antipodal points are also holomorphic.

However, given a choice of unit vector, $\vec{r}$, this condition is not satisfied for all choices of α_i. We show in Fig. 2.2 the allowed domain in the (α_1, α_2) plane for which the stability conditions Eq. (2.32) (and hence also the holomorphy conditions Eq. (2.29)) are satisfied, for two illustrative choices of the unit vector $\vec{r}$. The allowed region for $\vec{r} = (1/\sqrt{2}, 1/\sqrt{2})$ is shaded green and behind it (shaded blue) is the allowed region when $\vec{r} = (1/\sqrt{10}, 3/\sqrt{10})$. For both choices of $\vec{r}$, there is a kink in the allowed domain where it meets the line given by $\alpha_1 + \alpha_2 = 1$. At the kink, for all choices of $\vec{r}$, the potential is completely flat and vanishes in all directions in field space. The position of the kink can be calculated by solving the stability condition along this line:

$$\alpha_1 \;=\; \frac{r_1^2 - \sqrt{r_1^2 - r_1^4}}{2r_1^2 - 1}\,. \tag{2.33}$$

For the two examples shown in Fig. 2.2, $r_1 = 1/\sqrt{2}$ implies $\alpha_1 = 1/2$ at the kink, and $r_1 = 1/\sqrt{10}$ implies $\alpha_1 = 1/4$. In fact, because of the sign ambiguity, there are four unit vectors for each solution, corresponding to the ambiguous signs of r_1 and r_2.

Another projection of the domain of stability is shown in Fig. 2.3, which displays the allowed regions in the (α_1, r_1^2) plane for the fixed values $\alpha_2/\alpha_1 = 1, 2, 3, 5, 10$, as illustrated by the curves, respectively. Each pair of curves (red, green, purple, blue and black for increasing α_2/α_1) corresponds to the two equalities in Eq. (2.32), and the positivity inequalities are satisfied to the right of each pair of lines for a given value of α_2/α_1. For example, when $\alpha_2/\alpha_1 = 1$ (shown by the solid red curves), all values of r_1^2 are allowed if $\alpha_1 \geq 1$, while no values are allowed when $\alpha_1 < 1/2$. The point where the curves meet corresponds to the kink when $\alpha_1 = \alpha_2 = 1/2$ and $r_1^2 = 1/2$ that was seen in Fig. 2.2 where the green shaded region touches the black line. When $\alpha_2/\alpha_1 = 3$ (shown by medium dashed purple curves), the kink occurs when these two curves meet at $\alpha_1 = 1/4$

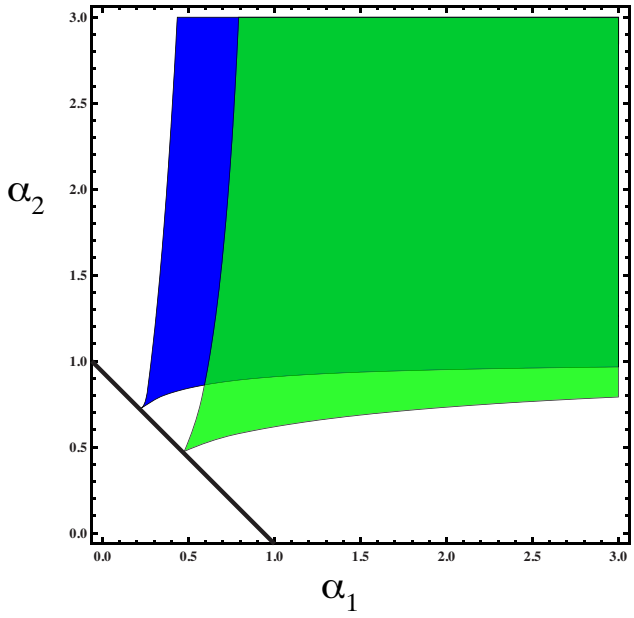

Figure 2.2: The shaded regions are the allowed values of α_1, α_2 for the illustrative choices $\vec{r} = (1/\sqrt{2}, 1/\sqrt{2})$ (green) and $\vec{r} = (1/\sqrt{10}, 3/\sqrt{10})$ (blue). There are kinks located at $(\alpha_1, \alpha_2) = (1/2, 1/2)$ and $(\alpha_1, \alpha_2) = (1/4, 3/4)$ for the two choices of unit vectors. The black line is $\alpha_1 + \alpha_2 = 1$. Reprinted with permission from [12].

and $r_1^2 = 1/10$.

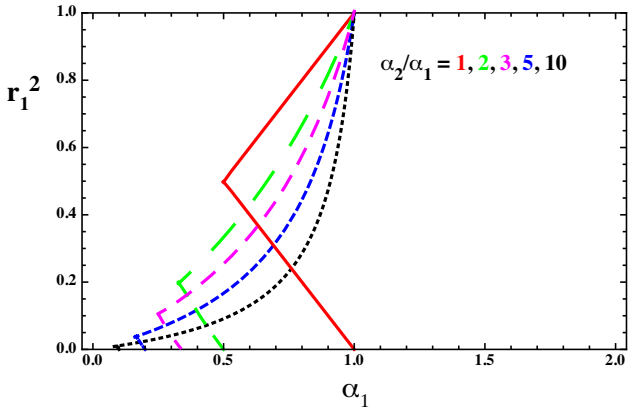

Figure 2.3: The allowed values of α_1, r_1^2 for fixed ratios of $\alpha_2/\alpha_1 = 1, 2, 3, 5, 10$. The two sets of curves are derived from the two constraint equations in Eq. (2.32). The stability inequality is satisfied for points with α_1 to the right of both curves of the same colour (red, green, purple, blue and black for increasing α_2/α_1). The point at which the two curves meet corresponds to the kink that appears in Fig 2.2 when $\alpha_1 + \alpha_2 = 1$. Reprinted with permission from [12].

The lower ellipse Eq. (2.27) in the (n_1, n_2) plane shown in Fig. 2.4 corresponds to this second example. As this corresponds to the position of the kink, only a single value of $r_1^2 = 1/10$ is allowed. The four red spots in the figure correspond to the four different vectors $\vec{r} = (\pm 1/\sqrt{10}, \pm 3/\sqrt{10})$. These four unit vectors correspond to four different superpotentials via the relation Eq. (2.28), which give $(n_1, n_2) = (3/4, 9/4), (3/4, 0), (0, 9/4), (0, 0)$. When $(\alpha_1, \alpha_2) = (1/4, 3/4)$, each of the four superpotentials defined by the pair n_i yields a true Minkowski solution. However, because we are at the kink, there are no other stable solutions.

Choosing a larger value of α_1 while keeping α_2/α_1 fixed would increase the allowed range in r_1^2 (as seen in Fig. 2.3) and would allow a continuum of stable Minkowski solutions along the real direction in field space. This is seen in the upper ellipse in Fig. 2.4, where we have chosen $\alpha_1 = 1/2$ and $\alpha_2 = 3/2$. In this case, the stability constraint, which can be read off Fig. 2.3 for $\alpha_2/\alpha_1 = 3$ at the chosen value of α_1, yields $r_1 < 1/2$. Unit vectors with $r_1 < 1/2$ correspond to arcs along the upper ellipse in Fig. 2.4. These are further shortened by the holomorphy requirement that $n_i \geq 0$, and the resulting allowed solutions are shown by the red arc segments in the upper ellipse.

To summarize this discussion of Minkowski solutions in the two-field case:

1) For any generic unit vector $\vec{r}$, there is always a kink in the boundary of the allowed values of (α_1, α_2) as shown in Fig. 2.2, and these kink solutions always satisfy $\alpha_1 + \alpha_2 = 1$ with α_1 given by Eq. (2.33). The kink solutions give a vanishing potential $V = 0$ in all directions in field space.

2) For any pair (α_1, α_2) satisfying $\alpha_1 + \alpha_2 = 1$, there are four unit vectors that are determined by inverting Eq. (2.33), namely

$$r_1 = \pm \frac{\alpha_1}{\sqrt{1 - 2\alpha_1 + 2\alpha_1^2}}. \tag{2.34}$$

The four values of the n_i that correspond to these choices are $(n_1, n_2) = (0, 0), (3\alpha_1, 0), (0, 3\alpha_2), (3\alpha_1, 3\alpha_2)$.

3) For $\alpha_1 + \alpha_2 > 1$, a continuum of stable Minkowski solutions exist and, when $\alpha_1 \geq 1$ with $\alpha_2/\alpha_1 \geq 1$, the entire ellipse (that is, all unit vectors $\vec{r}$) yield stable Minkowski solutions in the

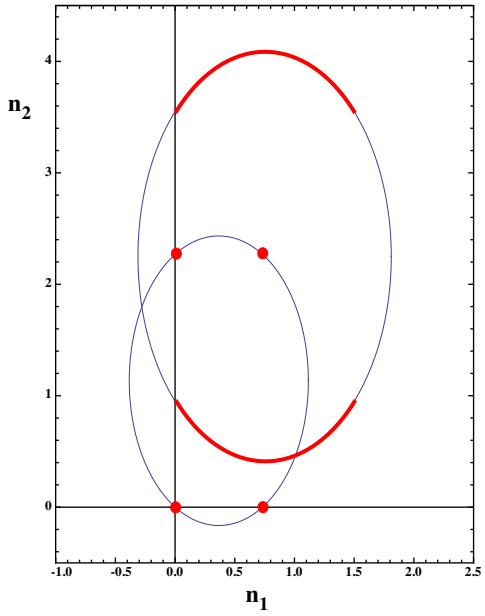

Figure 2.4: Minkowski solutions for $\alpha_1 = 1/4$, $\alpha_2 = 3/4$ (lower ellipse) and $\alpha_1 = 1/2$, $\alpha_2 = 3/2$ (upper ellipse). In the former case only the four red points corresponding to $\vec{r} = (\pm 1/\sqrt{10}, \pm 3/\sqrt{10})$ are allowed, whereas in the latter case the red arc segments correspond to allowed solutions. Reprinted with permission from [12].

real directions of field space.

4) The holomorphy conditions Eq. (2.29) are satisfied automatically if the stability conditions Eq. (2.32) are satisfied.

5) There is an infinite set of Minkowski solutions with positive integer powers of the fields in the superpotential.

2.3.2 De Sitter Solutions

We recall that in the single-field model we were able to construct a de Sitter solution by combining the two superpotentials corresponding to Minkowski solutions that can be visualized as opposite ends of a line segment. In the two-field model, we have a continuum of superpotentials that give Minkowski solutions, which are described by an ellipse Eq. (2.27). In this case it is possible to to construct new de Sitter solutions by combining superpotentials corresponding to antipodal

points on the ellipse Eq. (2.27). For example, consider the following combined superpotential:

$$W = a\ (\phi_1^{n_{1+}}\phi_2^{n_{2+}} - \phi_1^{n_{1-}}\phi_2^{n_{2-}})\ . \tag{2.35}$$

It is easy to see that the scalar potential in the real field direction is a de Sitter solution:

$$V\ =\ 3\cdot 2^{2-3\alpha_1-3\alpha_2}\cdot a^2 \tag{2.36}$$

in this case.

For the example described by the lower ellipse in Fig. 2.4, one example of a de Sitter solution is found by taking antipodal points corresponding to the red spots. When $\vec{r} = (1/\sqrt{10}, 3/\sqrt{10})$, we have $W = a(\phi_1^{3/4}\phi_2^{9/4} - 1)$, which is the unique solution with a holomorphic superpotential that results in a flat de Sitter potential in the real direction. However, as we discuss further below, this solution is actually not stable.

As an alternative example, we consider a two-field model with $\alpha_1 = 1$ and $\alpha_2 = 2$. The Minkowski solutions in this case are described by the ellipse Eq. (2.27) in (n_1, n_2) space shown in Fig. 2.5, whose centre is at $(3/2, 3)$. In this case, the entire ellipse can be used to construct de Sitter solutions, as all possible unit vectors $\vec{r}$ are allowed since $\alpha_1 > 1$ (see Fig. 2.3). As in the previous example, we can use antipodal points to construct de Sitter solutions, as illustrated in Fig. 2.5. One such pair of antipodal points is $(3, 3), (3, 0)$, corresponding to $\vec{r} = (1, 0)$, indicated by the horizontal orange line in Fig. 2.5. The corresponding superpotential is

$$W\ =\ a^2\ \left(\phi_1^3\phi_2^3 - \phi_2^3\right)\ , \tag{2.37}$$

so that the fields appear in the superpotential with positive integer powers. This example yields a de Sitter potential with the potential value

$$V\ =\ 3\cdot 2^{-7}\cdot a^2. \tag{2.38}$$

along the real field directions. A continuum of de Sitter solutions for real field values are possible for different choices of $\vec{r}$, e.g., the choice indicated in Fig. 2.5 by the blue line, all with the potential given by Eq. (2.38).

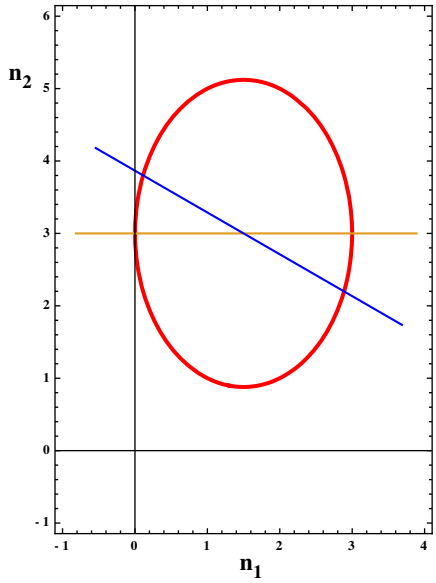

Figure 2.5: The Minkowski solutions for $\alpha_1 = 1$ and $\alpha_2 = 2$ are described by an ellipse in (n_1, n_2) space. Lines passing through the center of the ellipse connect antipodal points, as illustrated with two examples. Reprinted with permission from [12].

2.3.3 Stability Analysis

As in the single-field case, the de Sitter solutions of the two-field model require modification in order to be stable. Stable solutions can easily be found by deforming the Kähler potential to include stabilizing quartic terms:

$$K \;=\; -3\sum_{i=1}^{2}\alpha_i \ln(\phi_i + \phi_i^\dagger + b_i(\phi_i - \phi_i^\dagger)^4) : \; b_i \;>\; 0\,. \tag{2.39}$$

With this modification the potential along real field directions is still given by Eq. (2.36). To prove the stability of the two-field de Sitter solution with the quartic modification of the Kähler potential, we calculate the Hessian matrix $\partial^2 V/\partial y_i \partial y_j : i, j = 1, 2$ along the real field directions,

and demand that it be positive semi-definite. The Hessian matrix along the real field directions is of the form

$$a^2 \left(\frac{3.2^{1-3\alpha_1-3\alpha_2}}{\alpha_2 r_1^2 + \alpha_1 r_2^2} \right) \begin{bmatrix} x_1^{-2} A_1 & x_1^{-1} x_2^{-1} B \\ x_1^{-1} x_2^{-1} B & x_2^{-2} A_2 \end{bmatrix} , \tag{2.40}$$

where

$$A_1 \;=\; w^{-1} \left(\alpha_1^2 r_2^2 (1 + 4w + w^2) + \alpha_1 \alpha_2 r_1^2 (1 - w)^2 + \alpha_2 r_1^2 (96 b_1 x_1^3 - 1)(1 + w)^2 \right) , \tag{2.41}$$

$$A_2 \;=\; w^{-1} \left(\alpha_2^2 r_1^2 (1 + 4w + w^2) + \alpha_1 \alpha_2 r_2^2 (1 - w)^2 + \alpha_1 r_2^2 (96 b_2 x_2^3 - 1)(1 + w)^2 \right) , \tag{2.42}$$

$$B \;=\; -6 \alpha_1 \alpha_2 r_1 r_2 \, , \tag{2.43}$$

we have defined

$$w \;\equiv\; x_1^{\frac{3r_1}{\sqrt{\frac{r_1^2}{\alpha_1} + \frac{r_2^2}{\alpha_2}}}} \, x_2^{\frac{3r_2}{\sqrt{\frac{r_1^2}{\alpha_1} + \frac{r_2^2}{\alpha_2}}}} , \tag{2.44}$$

and the Hessian matrix is positive semi-definite if the condition

$$\mathcal{H} \;\equiv\; A_1 \, A_2 \;\geq\; B^2 \tag{2.45}$$

is satisfied.

The stability condition Eq. (2.45) for generic α_1, α_2, b_1, b_2 and $\vec{r}$ is

$$\begin{aligned} &\left(\alpha_1^2 r_2^2 (1 + 4w + w^2) + \alpha_1 \alpha_2 r_1^2 (1 - w)^2 + \alpha_2 r_1^2 (96 b_1 x_1^3 - 1)(1 + w)^2 \right) \\ &\times \left(\alpha_2^2 r_1^2 (1 + 4w + w^2) + \alpha_1 \alpha_2 r_2^2 (1 - w)^2 + \alpha_1 r_2^2 \left(96 b_2 \frac{w^{\frac{1}{r_2}\sqrt{\frac{r_1^2}{\alpha_1} + \frac{r_2^2}{\alpha_2}}}}{x_1^{(3r_1/r_2)}} - 1 \right) (1 + w)^2 \right) \\ &- 36 \alpha_1^2 \alpha_2^2 r_1^2 r_2^2 w^2 \;\geq\; 0 \, . \end{aligned} \tag{2.46}$$

A general stability analysis is intractable, so we have considered the simplified case: $\alpha_1 = \alpha_2 \equiv \alpha$

and $\vec{r} = (1/\sqrt{2}, 1/\sqrt{2})$, for which the positivity condition Eq. (2.45) becomes

$$\begin{aligned} &\left(2\alpha(1+w+w^2) + (96b_1x_1^3 - 1)(1+w)^2\right) \\ &\times \left(2\alpha(1+w+w^2) + (96b_2x_2^3 - 1)(1+w)^2\right) \;\geq\; 36\alpha^2 w^2\,. \end{aligned} \tag{2.47}$$

Eliminating x_2 in favour of x_1 and w via Eq. (2.44), this inequality becomes

$$\begin{aligned} &\left(2\alpha(1+w+w^2) + (96b_1x_1^3 - 1)(1+w)^2\right) \\ &\times \left(2\alpha(1+w+w^2) + \left(96b_2\frac{w\sqrt{2/\alpha}}{x_1^3} - 1\right)(1+w)^2\right) - 36\alpha^2 w^2 \;\geq\; 0\,. \end{aligned} \tag{2.48}$$

We note that $(96b_1x_1^3 - 1)$ dominates for $x_1 \gg 1$ and $\left(96b_2\frac{w\sqrt{2/\alpha}}{x_1^3} - 1\right)$ dominates for $x_1 \ll 1$, implying that there is an extremum for some intermediate value of x_1. This occurs at $x_1 = (b_2/b_1)^{1/6}\, w^{1/(3\sqrt{2\alpha})}$, and is a global extremum. Whether it is a maximum or a minimum depends on the sign of $2\alpha(1+w+w^2) - (1+w)^2$, and it is non-negative for

$$\alpha \geq \frac{2}{3}\,. \tag{2.49}$$

This is a necessary condition for the inequality Eq. (2.48) to be satisfied. We have not explored the full range of possible values of b_1 and b_2 when $\alpha_1 = \alpha_2 = \alpha$, but have checked that the stability condition Eq. (2.48) is always satisfied if $b_1 = b_2 = 1$ and $\alpha \geq 2/3$, irrespective of the value of w. We have also found that when $\alpha_1 \neq \alpha_2$ the sum $\alpha_1 + \alpha_2 \geq 4/3$.

We have also considered the case $\vec{r} = (0, 1)$ with $b_1 = b_2 = 1$. The inequality Eq. (2.46) reduces in this case to

$$\alpha_2(1-w)^2 + (1+w)^2(96w^{1/\sqrt{\alpha_2}} - 1) \;\geq\; 0\,, \tag{2.50}$$

which is always satisfied for $\alpha_2 \;\geq\; 1$. It is easy to check that the same is true for the case $\vec{r} = (1, 0)$. Based on these cases and the previous example with $\vec{r} = (1/\sqrt{2}, 1/\sqrt{2})$, we expect that

there are generic stable solutions for a range of $\vec{r}$ in the first and third quadrants where $r_1/r_2 > 0$. However, the situation is different when $r_1/r_2 < 0$. We find that the inequality Eq. (2.45) cannot be satisfied for $\vec{r} = (-1/\sqrt{2}, 1/\sqrt{2})$ and $b_1 = b_2 = 1$, so there are no stable de Sitter solutions, and we expect the same to be the case for other choices of $\vec{r}$ in the second or fourth quadrant.

In summary, we have established the existence of stable de Sitter solutions only when $\vec{r}$ is in either first or third quadrant.

2.4 N-field models

Finally, we generalize the above set of examples to models with multiple fields $N > 2$.

2.4.1 Minkowski Solutions

The natural generalization of the Kähler potential in Eq. (2.24) is simply a sum of N similar terms:

$$K \;=\; -3\sum_{i=1}^{N}\alpha_i \ln(\phi_i + \phi_i^\dagger)\,. \tag{2.51}$$

Similarly, we adopt the following ansatz for the superpotential:

$$W \;=\; a\prod_{i=1}^{N}\phi_i^{n_i}\,, \tag{2.52}$$

in which case the potential along the real field directions x_i is

$$V \;=\; \left(\sum_{i=1}^{N}\frac{(2n_i - 3\alpha_i)^2}{3\alpha_i} - 3\right)\cdot a^2 \cdot \left(\prod_{i}^{N} 2^{-3\alpha_i} x_i^{2n_i - 3\alpha_i}\right)\,. \tag{2.53}$$

We can obtain Minkowski solutions along the real field directions by setting

$$\sum_{i=1}^{N}\frac{(2n_i - 3\alpha_i)^2}{3\alpha_i} \;=\; 3\,, \tag{2.54}$$

which describes an ellipsoid in $(n_1, ..., n_N)$ space whose centre is at $(3\alpha_1/2, ..., 3\alpha_N/2)$. Once again we find a continuum of Minkowski solutions. The points on the ellipsoid can be parametrized

conveniently using an N-dimensional unit vector $\vec{r}$:

$$n_i \;=\; \frac{3}{2}\left(\alpha_i + \frac{r_i}{\sqrt{\sum_{j=1}^{N}\frac{r_j^2}{\alpha_j}}}\right) \qquad i=1,...,N; \quad r_1^2+...+r_N^2=1\,, \tag{2.55}$$

where the unit vector $\vec{r}$ is to be considered as anchored at the centre of the ellipsoid. To ensure holomorphy of the superpotential we need $n_i \geq 0$, and the masses of the imaginary field components y_i are given by

$$m_{y_i}^2 \;=\; \frac{2^{2-3(\sum\alpha_i)}}{\alpha_i^2}\cdot\left(\alpha_i^2 - \frac{r_i^2}{\left(\sum_{j=1}^{N}\frac{r_j^2}{\alpha_j}\right)}\right)\cdot a^2\cdot\prod_{j=1}^{N}x_j^{2n_j-3\alpha_j}, \qquad i=1,...,N\,. \tag{2.56}$$

For stability, we impose conditions similar to Eq. (2.32), namely:

$$\alpha_i^2 - \frac{r_i^2}{\left(\sum_{j=1}^{2}\frac{r_j^2}{\alpha_j}\right)} \;\geq\; 0 \qquad i=1,...,N\,. \tag{2.57}$$

As in two-field models, ensuring these stability conditions are satisfied implies that the holomorphy conditions are also satisfied. For a given unit vector $\vec{r}$, one can ask what values of $\alpha_1,...,\alpha_N$ satisfy the stability conditions. We find a multidimensional region analogous to that in Fig. 2.2, with a vertex that satisfies $\alpha_1+...+\alpha_N=1$. We show in Fig. 2.6 the allowed region of α_1,α_2 and α_3 for a three-field model with $\vec{r}=(1/\sqrt{3},1/\sqrt{3},1/\sqrt{3})$.

The vertex is a special solution that corresponds to $V=0$ in both the real and imaginary field directions. When the sign of one of the components of $\vec{r}$ is changed, the region in $\alpha_1,...,\alpha_N$ space that satisfies Eq. (2.57) remains the same. Therefore, there are 2^N unit vectors, each differing only in the sign of the components, that have the same vertex solution.

The above observations on the vertex solution can be summarized as follows. When

$$\sum_{i=1}^{N}\alpha_i \;=\; 1\,, \tag{2.58}$$

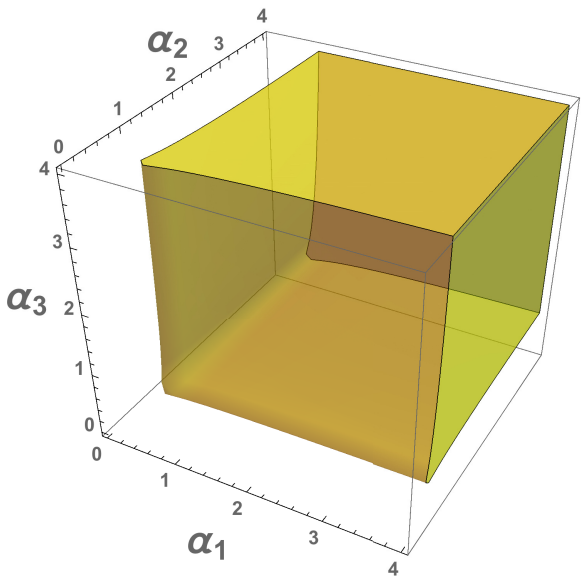

Figure 2.6: Allowed values of $\alpha_1, \alpha_2, \alpha_3$ for a three-field model with $\vec{r} = (1/\sqrt{3}, 1/\sqrt{3}, 1/\sqrt{3})$. Reprinted with permission from [12].

there are 2^N superpotentials of the form

$$W \;=\; a\,\phi_{i_1}^{3\alpha_{i_1}} ... \phi_{i_n}^{3\alpha_{i_n}}\,, \tag{2.59}$$

where $\{i_1, ..., i_n\}$ $(n \leq N)$ is a subset of $\{1, 2, ..., N\}$, that all give $V = 0$ in both the real and imaginary field directions.

2.4.2 De Sitter Solutions

Finally we discuss de Sitter solutions in N-field models. Here the Kähler potential is again given by

$$K \;=\; -3 \sum_{i=1}^{N} \alpha_i \ln(\phi_i + \phi_i^\dagger)\,, \tag{2.60}$$

and, as in the two-field case, the superpotential may be constructed from two antipodal points of the ellipse Eq. (2.54):

$$W \;=\; a \left(\prod_{i=1}^{N} \phi_i^{n_{i+}} - \prod_{i=1}^{N} \phi_i^{n_{i-}} \right)\,, \tag{2.61}$$

where the exponents are given by

$$n_{i\pm} \;=\; \frac{3}{2}\left(\alpha_i \pm \frac{r_i}{\sqrt{\sum_{j=1}^{N}\frac{r_j^2}{\alpha_j}}}\right) \qquad i=1,...,N; \quad r_1^2+...+r_N^2=1\,, \tag{2.62}$$

and the potential along the real field directions is then

$$V \;=\; 3\cdot 2^{(2-3\sum_{i=1}^{N}\alpha_i)}\cdot a^2\,. \tag{2.63}$$

We use a simple three-field model with $\alpha_1 = 2$, $\alpha_2 = 2$ and $\alpha_3 = 4$ for illustration. The Minkowski solutions are described by an ellipsoid in (n_1, n_2, n_3) space centred at $(3, 3, 6)$, which is shown in Fig. 2.7.

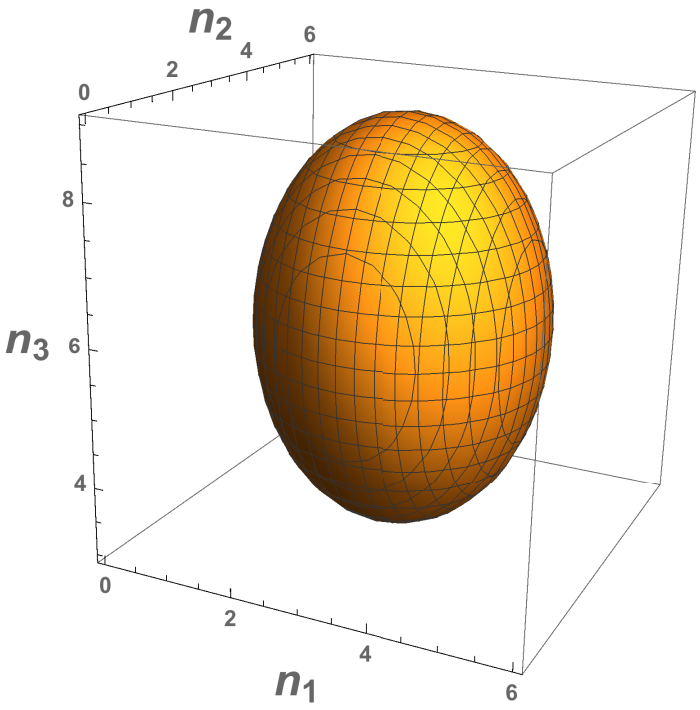

Figure 2.7: Minkowski solutions for the three-field model with $\alpha_1 = 2$, $\alpha_2 = 2$ and $\alpha_3 = 4$. Reprinted with permission from [12].

To construct de Sitter solutions for this model, we choose the antipodal points $(3,3,9),(3,3,3)$ corresponding to the unit vector $\vec{r}=(0,0,1)$, which yield the superpotential:

$$W \;=\; a\,(\phi_1^3\phi_2^3\phi_3^9 - \phi_1^3\phi_2^3\phi_3^3)\,. \tag{2.64}$$

This yields a de Sitter potential along the real field directions with potential

$$V \;=\; 3\cdot 2^{-16}\cdot a^2\,. \tag{2.65}$$

2.4.3 Stability Analysis

The stability analysis of the de Sitter solution in the N-field model is difficult, as it requires finding the eigenvalues of an $N\times N$ matrix. However, as in the two-field model, we do not expect the solution to be stable unless the Kähler potential is deformed, e.g., to

$$K \;=\; -3\sum_{i=1}^{N}\alpha_i \ln(\phi_i+\phi_i^\dagger + b_i(\phi_i-\phi_i^\dagger)^4)\,. \tag{2.66}$$

With this modification, for any given unit vector $\vec{r}$ there should exist a region in $(\alpha_1,...,\alpha_N)$ space where the de Sitter solution is stable.

To demonstrate this in a specific three-field example, we consider the model with three chiral fields S,T,U that was considered in [21]. This model is defined by the following Kähler potential and superpotential:

$$\begin{aligned} K &= -\ln(S+S^\dagger) \;-\; 3\ln(T+T^\dagger) \;-\; 3\ln(U+U^\dagger)\,,\\ W &= W(S,T,U)\,. \end{aligned} \tag{2.67}$$

This model is of particular interest as it arises in the compactification of Type IIB string theory on $T^6/Z_2\times Z_2$. Then the three chiral fields are the axiodilaton S, a volume modulus T and a complex structure modulus U. One expects that the perturbative contribution to the superpotential should be a polynomial and that the non-perturbative contribution would have a decaying exponential

form. For our analysis we assume that the powers of the fields in the superpotential could also be fractional. In our notations, this STU model has $\alpha_1 = 1/3, \alpha_2 = 1$ and $\alpha_3 = 1$.

We first construct a Minkowski solution. We can use the stability conditions to find a unit vector $\vec{r}$ and construct an appropriate superpotential. One such unit vector is $\vec{r} = (0, 1, 0)$. This leads to a superpotential of the form

$$W \;=\; aS^{1/2}T^3U^{3/2}\,, \tag{2.68}$$

which gives a stable Minkowski solution $V = 0$ along real field directions [7].

In order to construct de Sitter solutions we add stabilization terms to the Kähler potential:

$$K \;=\; -\ln(S+S^\dagger+b_S(S-S^\dagger)^4) \,-\, 3\ln(T+T^\dagger+b_T(T-T^\dagger)^4) \,-\, 3\ln(U+U^\dagger+b_U(U-U^\dagger)^4)\,. \tag{2.69}$$

As discussed above, we use antipodal points to construct the superpotential, choosing $\vec{r} = (0, \pm 1, 0)$, in which case:

$$W \;=\; a\,S^{1/2}U^{3/2}(T^3-1)\,. \tag{2.70}$$

With this we get a de Sitter solution along the real field directions with potential

$$V \;=\; \frac{3}{32}\cdot a^2\,. \tag{2.71}$$

In order to check whether the de Sitter solution is stable for the antipodal points that we have chosen, we calculate the Hessian matrix along the real field directions to verify that the eigenvalues are non-negative. Defining

$$S \;=\; s+iy_1\,, \qquad T \;=\; t+iy_2\,, \qquad U \;=\; u+iy_3\,, \tag{2.72}$$

[7] We mention in passing that the STU model does not admit any superpotential with only integer powers, for either Minkowski or de Sitter solutions.

we calculate the Hessian matrix $\partial^2 V/\partial y_i \partial y_j : i,j = 1,2,3$ along the real field directions, finding

$$\begin{bmatrix} \frac{a^2(1+4t^3+t^6)}{64s^2t^3} & 0 & 0 \\ 0 & \frac{-3a^2+72a^2b_T(1+t^3)^2}{16t^2} & 0 \\ 0 & 0 & \frac{3a^2(1+4t^3+t^6)}{64t^3u^2} \end{bmatrix} . \tag{2.73}$$

We see that the Hessian matrix is diagonal, so the eigenvalues are simply the diagonal entries. For the Hessian matrix to be positive semi-definite we need

$$-3a^2 + 72a^2\, b_T\, (1+t^3)^2 \;\geq\; 0\,, \tag{2.74}$$

which is independent of b_S and b_U. Therefore, we simply need

$$b_T \;\geq\; \frac{1}{24}\,, \tag{2.75}$$

with no restriction on b_S and b_U.

2.5 Summary

Generalizing previous discussions of de Sitter solutions in single-field no-scale models [8, 16, 19], in this chapter we have discussed de Sitter solutions in multi-field no-scale models as may appear in realistic string compactifications with multiple moduli.

As a preliminary, we showed that the space of Minkowski vacua in multi-field no-scale models is characterized by the surface of an ellipsoid. The parameters in these models are the coefficients $(\alpha_1, ..., \alpha_N)$ in the generalized no-scale Kähler potential and a unit vector $\vec{r}$ that selects a particular pair of antipodal points on this ellispoid whose center is located at $(3\alpha_1/2, ..., 3\alpha_N/2)$. Requiring the stability of Minkowski solutions for a fixed $\vec{r}$ leads us to a region in $(\alpha_1, ..., \alpha_N)$ space with a vertex that is a special point where $\sum_{i=1}^N \alpha_i = 1$. Such points describe Minkowski vacua with potentials that are flat in both the real and imaginary field directions. In this way we constructed 2^N monomial (in each field) superpotentials for models with $\sum_{i=1}^N \alpha_i = 1$ that yield acceptable

Minkowski vacua. The exponent of each monomial is determined by the coefficients α_i and the vectors, r_i.

We then constructed de Sitter solutions by combining the superpotentials at antipodal points, generalizing a construction given originally in the single-field case in [8]. These de Sitter solutions are unstable if the simple no-scale Kähler potential is used, and require stabilization. We showed that modifying the Kähler potential with a quartic term stabilizes a specific two-field model with $\alpha_1 = \alpha_2 = \alpha$ and $\vec{r} = (1/\sqrt{2}, 1/\sqrt{2})$ for $\alpha \geq 2/3$, and we expect the stability to hold for other generic $\vec{r}$ for suitable ranges of α_1, α_2. We also expect that similar stable de Sitter solutions exist for N-field models under certain conditions, as demonstrated explicitly in a specific three-field model motivated by the compactification of Type IIB string theory [21].

We note that satisfying the stability requirement also ensures that the superpotential is holomorphic in the Minkowski case, i.e., contains only positive powers of the chiral fields, whereas this is not necessarily true in the de Sitter case. It is easy to find infinite discrete series of models for which these powers are integral, and we have provided a number of illustrative single- and multi-field examples.

3. FROM DE SITTER TO INFLATIONARY MODELS[1]

3.1 Introduction

In the previous chapter, we discussed Minkowski and de Sitter solutions within the 4d $\mathcal{N} = 1$ no-scale supergravity framework. Several issues then arise within this broader theoretical context. How unique are no-scale supergravity models with Minkowski or de Sitter solutions? What are the relationships between them? What other geometrical interpretations are possible? Can the de Sitter models be used to construct inflationary models predicting perturbations that are consistent with observations, e.g., resembling the successful [29, 30] predictions of the Starobinsky model [31] as in [32]? How may the universe evolve from a (near-)de Sitter inflationary state towards the (near-)Minkowski contemporary epoch with its (small) cosmological constant, a.k.a. dark energy?

Aspects of these questions have been addressed previously in a series of papers. In [12], we constructed dS vacua in two- and multifield models as could occur in string compactifications, discussed the conditions for their stability, and gave examples with only integer powers of the chiral fields in the superpotential. There is a long history of no-scale supergravity models of inflation [33, 34, 35, 36], but only recently has it been realized that simple forms of the superpotential can yield Starobinsky-like inflation [16, 19, 32, 37, 38, 39, 40, 41, 42, 43, 44, 45, 46, 47, 48, 49, 50]. Indeed, there are several forms for the superpotential based on two chiral fields [37]. In [38] a general discussion of two-field no-scale supergravity models of inflation yielding predictions similar to those of the Starobinsky model and using the non-compact SU(2,1)/SU(2)$\times$U(1) symmetry to catalogue them in six equivalence classes was presented. In [39] a specific minimal SU(2,1)/SU(2)$\times$U(1) no-scale model that incorporates Starobinsky-like inflation, supersymmetry breaking and dark energy was constructed. This construction was generalized in [40] to inflationary models based on generalized no-scale structures with different values of the Kähler curvature R, as may occur if different numbers of complex moduli contribute to driving inflation.

[1]Reprinted with permission from "From Minkowski to de Sitter in Multifield No-Scale Models" by J. Ellis, B. Nagaraj, D. V. Nanopoulos, K. A. Olive and S. Verner, 2019, Springer Nature, JHEP 10, 161 (2019). Copyright [2019] by the authors.

In this chapter we discuss the uniqueness of superpotentials leading to Minkowski, dS and AdS vacua of single-field no-scale supergravity models, and how pairs of Minkowski superpotentials can be used to construct dS/AdS solutions. Expanding on previous work which showed how this construction may be extended to two- and multifield no-scale supergravity models, we show how matter fields can be incorporated in a multifield construction of Minkowski, dS and AdS vacua. We also provide a geometrical visualization of the construction. We also mention how Starobinsky-like inflationary models can be constructed in this framework, and comment on the inclusion of additional twisted or untwisted moduli fields.

The structure of this chapter is as follows. In Section 3.2 we first review the of structure no-scale supergravity and previous work within that framework. We then discuss the uniqueness of single-field monomial superpotentials leading to a Minkowski vacuum and how they can be combined in pairs to yield dS vacua. Section 3.3 shows how these constructions can be extended to multiple moduli, and introduces a geometrical interpretation. Section 3.4.1 then further extends these constructions to include untwisted matter fields, and Section 3.4.2 considers the case of twisted matter fields. This is followed in Section 3.5 by a discussion of inflationary models with either untwisted or twisted matter fields. Finally, our results are summarized in Section 3.6.

3.2 Vacua Solutions with Moduli Fields

3.2.1 No-Scale Supergravity Framework

We first recall some general properties of no-scale supergravity models, which emerge naturally from generic string compactifications in the low-energy effective limit [11]. The simplest $\mathcal{N} = 1$ no-scale supergravity models were first considered in [6, 7] and are characterized by the following Kähler potential [8]:

$$K \;=\; -3\,\ln(T+\overline{T}), \tag{3.1}$$

where field T is a complex chiral field that can be identified as the volume modulus field, and $\overline{T}$ is its conjugate field. The minimal no-scale Kähler potential Eq. (3.1) describes a non-compact $\frac{SU(1,1)}{U(1)}$ coset manifold and its higher-dimensional generalizations [9] will be considered in the

following sections. Furthermore, the Kähler curvature of a general Kähler manifold is given by the expression $R_{i\bar{j}} \equiv \partial_i \partial_{\bar{j}} \ln K_{i\bar{j}}$, and the scalar curvature obeys the relation:

$$R \equiv \frac{R_{i\bar{j}}}{K_{i\bar{j}}}, \tag{3.2}$$

where $K_{i\bar{j}}$ is the inverse Kähler metric. If we consider the maximally-symmetric $\frac{SU(1,1)}{U(1)}$ Kähler manifold (3.1), the Kähler curvature reduces to the familiar result $R = \frac{2}{3}$. The Kähler potential Eq. (3.1) can be modified by introducing a curvature parameter α:

$$K = -3\,\alpha\,\ln(T + \overline{T}), \tag{3.3}$$

which also parametrizes a non-compact $\frac{SU(1,1)}{U(1)}$ coset manifold, but with a positive constant curvature $R = \frac{2}{3\alpha}$ if we assume that $\alpha > 0$. This unique structure was first discussed in [8], and similar models were studied in [16, 51, 52], where they were termed α-attractors.

To account for interactions, the Kähler potential is extended by including a superpotential W:

$$G \equiv K + \ln W + \ln \overline{W}\,, \tag{3.4}$$

yielding the effective scalar potential:

$$V = e^G \left[\frac{\partial G}{\partial \Phi_i} K_{i\bar{j}} \frac{\partial G}{\partial \bar{\Phi}_{\bar{j}}} - 3 \right], \tag{3.5}$$

where the fields Φ_i are complex scalar fields, $\bar{\Phi}_{\bar{i}}$ are their conjugate fields, and $K_{i\bar{j}}$ is the inverse Kähler metric. For more on $N = 1$ supergravity models, see [24].

3.2.2 Review of Earlier Work

As was shown in [8, 16, 19], one can consider combining cubic and constant superpotential terms to acquire a de Sitter vacuum solution. Choosing the following superpotential form:

$$W = 1 - T^3, \tag{3.6}$$

together with the Kähler potential Eq. (3.1), and imposing the condition $T = \overline{T}$, the effective scalar potential Eq. (3.5) yields a de Sitter vacuum solution $V = \frac{3}{2}$. However, the superpotential Eq. (3.6) leads to an unstable vacuum solution, since the mass-squared of the imaginary component of the scalar field is negative: $m^2_{Im\,T} = -2$. As we discuss in more detail below, the problem of instabilities can be addressed by adding a quartic term to the Kähler potential [20, 37, 40].

A detailed analysis of the general de Sitter vacua constructions for multi-moduli models was conducted in [12] and for convenience, we recall some of the key results. The Minkowski vacua solutions for a single complex chiral field T were found by considering the Kähler potential Eq. (3.3) with a monomial superpotential of the following form:

$$W = \lambda \cdot T^{n_\pm}\,, \tag{3.7}$$

where $n_\pm$ are two possible solutions given by:

$$n_\pm = \frac{3}{2}\left(\alpha \pm \sqrt{\alpha}\right)\,. \tag{3.8}$$

Along the real T direction, $V = 0$. The scalar mass-squared in the imaginary direction is:

$$m^2_{Im\,T} = 2^{2-3\alpha} \cdot \lambda^2 \cdot \frac{(\alpha - 1)}{\alpha} \cdot T^{\pm 3\sqrt{\alpha}}\,, \tag{3.9}$$

where the choice $T^{\pm 3\sqrt{\alpha}}$ corresponds to the two possible solutions $n_\pm$ Eq. (3.8). As can be seen from Eq. (3.9), in order to obtain a stable Minkowski vacuum solution, the stability condition

$\alpha \geq 1$ has to be satisfied. For cases when $0 < \alpha < 1$, quartic stabilization terms in the imaginary direction must be introduced in the Kähler potential Eq. (3.3).

As was shown in [8, 12, 40], de Sitter vacua solutions can be obtained from the Kähler potential Eq. (3.3) by choosing a superpotential of the form:

$$W = \lambda_1 T^{n_-} - \lambda_2 T^{n_+}\,, \tag{3.10}$$

where $n_\pm$ is given by Eq. (3.8). In this case, along the real T direction the effective scalar potential Eq. (3.5) becomes:

$$V = 3 \cdot 2^{2-3\alpha} \cdot \lambda_1 \lambda_2. \tag{3.11}$$

One of the most fascinating features of the de Sitter vacua construction Eq. (3.10) is that it is obtained by combining two distinct Minkowski vacua solutions Eq. (3.7). In the next sections, we will show that there is a deeper connection between dS/AdS and Minkowski vacua solutions and that this relation is not accidental.

Superpotential classes yielding constant scalar potentials were first considered in [8], namely:

$$1) \qquad W = \lambda \qquad \text{with} \qquad \alpha = 1\,, \tag{3.12}$$

$$2) \qquad W = \lambda T^{3\alpha/2}\,, \tag{3.13}$$

$$3) \qquad W = \lambda T^{3\alpha/2}(T^{3\sqrt{\alpha}/2} - T^{-3\sqrt{\alpha}/2})\,. \tag{3.14}$$

Comparing solution 1) to Eq. (3.10), we see that it can be recovered by setting $\alpha = 1$, $\lambda_1 = \lambda$ and $\lambda_2 = 0$. Because λ_2 is chosen to be zero, we find a Minkowski vacuum: $V = 0$. Solution 3) is identical to Eq. (3.10) with $\lambda_1 = \lambda_2 = -\lambda$. Solution 2) can also be obtained from Eq. (3.10) with the aid of a Kähler transformation:

$$K \to K + f(T) + \bar{f}(\overline{T}) \tag{3.15}$$

and

$$W(T) \longrightarrow \widetilde{W}(T) = e^{-f(T)} W(T), \tag{3.16}$$

with

$$f(T) = \ln\left(\frac{1+T^{3\sqrt{\alpha}}}{2T^{3\sqrt{\alpha}/2}}\right), \tag{3.17}$$

and applying the transformation laws Eq. (3.15), Eq. (3.16) with Eq. (3.17) and $\lambda_1 = -\lambda_2 = \lambda/2$, we recover solution 2) which is in fact an AdS vacuum solution $V = -(3/2^{3\alpha})\,\lambda^2$, which is always negative.

While the scalar potential is flat in the real direction, the scalar mass-squared of the imaginary component is given by:

$$m^2_{Im\,T} = \frac{2^{2-3\alpha}\left[\lambda_1^2(\alpha-1)T^{-3\sqrt{\alpha}} - 2\lambda_1\lambda_2(\alpha+1) + \lambda_2^2(\alpha-1)T^{3\sqrt{\alpha}}\right]}{\alpha}, \tag{3.18}$$

For $\alpha > 0$, in the absence of stabilization terms, there are always some field values for which the instability in the imaginary direction persists. The problem of instability can be remedied by modifying the Kähler potential Eq. (3.3) and introducing quartic stabilization terms in the imaginary direction [20, 37, 40]:

$$K = -3\,\alpha \ln\left(T + \overline{T} + \beta\,(T-\overline{T})^4\right), \tag{3.19}$$

with $\beta > 0$. The newly-introduced quartic stabilization term does not alter the potential in the real direction, while it stabilizes the mass of the imaginary component Eq. (3.18) so that:

$$m^2_{Im\,T} = \frac{2^{2-3\alpha}\left[\lambda_1^2(\alpha-1+96\beta T^3)T^{-3\sqrt{\alpha}} - 2(\alpha+1-96\beta T^3)\lambda_1\lambda_2 + \lambda_2^2(\alpha-1+96\beta T^3)T^{3\sqrt{\alpha}}\right]}{\alpha}. \tag{3.20}$$

3.2.3 Uniqueness of Vacua Solutions

By solving an inhomogeneous differential equation, we now show that the monomial Minkowski superpotential solutions Eq. (3.7) are the only possible unique solutions that yield $V = 0$, while

the combination of two distinct Minkowski solutions Eq. (3.10) yield dS/AdS vacuum solutions.

We consider a general superpotential expression $W(T)$, which is a function of volume modulus T only, and solve the general homogeneous differential equation, which is equivalent to finding Minkowski vacuum solutions. As before, we assume that the Vacuum Expectation Value (VEV) of the imaginary component $\langle Im\, T\rangle = 0$, so that $T = \overline{T}$ and $W(T) = \overline{W}(\bar{T})$. Using the Kähler potential Eq. (3.3) and the effective scalar potential Eq. (3.5), we find

$$V = (2T)^{-3\alpha} \cdot \left[\frac{(3\alpha W - 2TW')^2}{3\alpha} - 3W^2 \right], \tag{3.21}$$

where $W \equiv W(T)$ and $W' \equiv \frac{dW(T)}{dT}$. In order to find Minkowski vacuum solutions, we set Eq. (3.21) to zero:

$$\frac{(3\alpha W - 2TW')^2}{3\alpha} - 3W^2 = 0. \tag{3.22}$$

Solving the homogeneous differential equation Eq. (3.22), we obtain two distinct Minkowski solutions:

$$W = \lambda_i \cdot T^{\frac{3}{2}\left(\alpha \pm \sqrt{\alpha}\right)}, \tag{3.23}$$

where λ_i is an arbitrary constant. To find the dS/AdS vacuum solutions, we set the differential equation Eq. (3.21) equal to a constant and solve the following inhomogeneous equation:

$$\frac{(3\alpha W - 2TW')^2}{3\alpha} - 3W^2 = \Lambda \cdot (2T)^{3\alpha}, \tag{3.24}$$

where Λ is an arbitrary constant. We look for a particular superpotential solution to the inhomogeneous equation Eq. (3.24) of the following form:

$$W = \lambda_1 \cdot T^{\frac{3}{2}\left(\alpha \pm \sqrt{\alpha}\right)} - \lambda_2 \cdot T^{m}. \tag{3.25}$$

Inserting the expressions Eq. (3.25) into Eq. (3.24), we find that $m = n_{\mp} = \frac{3}{2}\left(\alpha \mp \sqrt{\alpha}\right)$ is a particular solution of the inhomogeneous differential equation and the general solution has the

following form:

$$W = \lambda_1 \cdot T^{n_\pm} - \lambda_2 \cdot T^{n_\mp}, \text{ with } \quad V = \Lambda\,, \tag{3.26}$$

where we have defined the constant $\Lambda = 3 \cdot 2^{2-3\alpha} \cdot \lambda_1\,\lambda_2$. Thus, we have constructed the unique combination of two Minkowski solutions that yields dS/AdS solutions [2].

3.2.4 Generalized Solutions and Vacuum Stability

Before concluding this section, we introduce a formalism with which the construction of Minkowski-dS-AdS solutions can be generalized and applied to more complicated Kähler manifolds. Let us write:

$$K = -3\,\alpha \ln(\mathcal{V})\,, \tag{3.27}$$

where $\mathcal{V}$ is the argument inside the logarithm. For the simplest minimal no-scale $\frac{SU(1,1)}{U(1)}$ supergravity case with a single volume modulus field T, we have $\mathcal{V} \equiv T + \overline{T}$. As before, and in all the cases that we consider, we assume that the VEV of the imaginary part of the complex field is fixed to zero: $\langle Im\, T\rangle = 0$, which can always be achieved by introducing quartic stabilization terms in Eq. (3.27).

For the single field case, the effective scalar potential Eq. (3.5) becomes:

$$V = \frac{\hat{V}}{\mathcal{V}^{3\alpha}}, \text{ with } \quad \hat{V} = \frac{|\mathcal{V} \cdot \overline{W}_{\overline{T}} - 3\alpha W|^2}{3\alpha} - 3|W|^2. \tag{3.28}$$

In the real direction, where $T = \overline{T}$, we define:

$$\mathcal{V} \longrightarrow \xi, \tag{3.29}$$

so that the argument inside the logarithm becomes $\xi = 2T$.

From our previous discussion, we already know which superpotential forms reduce to Minkowski solutions. We introduce the following notation, which will be used for all our Kähler coset mani-

[2] We note that these solutions correspond to flat directions in the real field direction. It is possible and relatively straightforward to construct minima with non-zero vacuum energy. In particular, it is well known that supergravity models with unbroken supersymmetry generally lead to AdS vacua.

folds [3] :

$$W_M \equiv \lambda \cdot \xi^{n_\pm}, \text{ with } \quad V = 0\,, \tag{3.30}$$

where, as usual, the two possible choices $n_\pm$ are given by Eq. (3.8). Note that, for this construction to work, we must impose the constraint $\xi > 0$ and the positive curvature condition $\alpha > 0$, which are necessary features of the no-scale structure [4].

With this redefinition, the scalar mass-squared in the imaginary field direction given in Eq. (3.9) becomes:

$$m^2_{Im\,T} = \frac{4\,\lambda^2(\alpha-1)\xi^{\pm 3\sqrt{\alpha}}}{\alpha}\,, \tag{3.31}$$

where the sign depends on the choice of the Minkowski vacuum solution in Eq. (3.30). We will later show that the same Minkowski mass expression Eq. (3.31) holds for any Kähler potential form, and hence that the solution is stable when $\alpha \geq 1$. When $0 < \alpha < 1$, Minkowski vacuum solutions become unstable and we must introduce the quartic stabilization terms in the imaginary direction.

Similarly, dS/AdS vacua solutions are constructed by combining two different Minkowski solutions Eq. (3.30),

$$W_{dS/AdS} = \lambda_1 \cdot \xi^{n_-} - \lambda_2 \cdot \xi^{n_+}\,, \tag{3.32}$$

and we call such constructions Minkowski pairs. The dS/AdS vacuum solution Eq. (3.32) yields an effective scalar potential Eq. (3.5):

$$V = 12\,\lambda_1\,\lambda_2\,, \tag{3.33}$$

which allows three different types of vacua:

- de Sitter vacuum solutions when λ_1 and λ_2 are $\neq 0$ and have the same sign.

[3] Note that we are using a trick in our definition of the superpotential. Strictly speaking, ξ is defined by the argument of the $\log$ in K when all fields are taken as real. However in the superpotential we are assuming that ξ is a function of (complex) superfields and ignore the restriction to real fields.

[4] Note also that the definition of λ here differs from that in Eq. (3.7) by a constant factor of $2^{n_\pm}$.

- anti-de Sitter vacuum solutions when λ_1 and λ_2 are $\neq 0$ and have opposite signs.

- Minkowski vacuum solutions when either λ_1 or λ_2 is set to zero.

The generalization of the scalar mass in the imaginary direction $m^2_{Im\,T}$ in Eq. (3.18) is given by:

$$m^2_{Im\,T} = \frac{4\left[\lambda_1^2(\alpha-1)\xi^{-3\sqrt{\alpha}} - 2(\alpha+1)\lambda_1\lambda_2 + \lambda_2^2(\alpha-1)\xi^{3\sqrt{\alpha}}\right]}{\alpha}\,, \tag{3.34}$$

which should always be positive, $m^2_{Im\,T} \geq 0$ for stability in the imaginary field direction. Recalling that dS vacuum solutions are acquired when λ_1 and λ_2 have the same sign, we introduce the ratio coefficient $\gamma = \lambda_1/\lambda_2$, which must always be positive.

To visualize this condition, we plot in Fig. 3.1 the (α, γ) plane with T on the vertical axis, and the size of $\log\left(m^2_{Im\,T}/4\,\lambda_2^2\right)$ indicated by color coding. The boundary of the colored region corresponds to the critical value of $m^2_{Im\,T}/4\,\lambda_2^2 = 0$, and it indicates when $m^2_{Im\,T}$ becomes unstable. Interestingly, the same general expression Eq. (3.34) holds also for more complicated forms of ξ. It is important to note that Fig. 3.1 shows two colored regions which are separated by a gap, and indicates that the dS vacuum becomes unstable in the imaginary direction for certain values of T and α.

To understand the occurrence of the dS vacuum instability, we consider two specific cases with different values of α, where for illustrative purposes we choose $\lambda_1 = \lambda_2 = 1$, and we use the field parametrization $T = (x + iy)/\sqrt{2}$. The effective scalar potential is plotted in Fig. 3.2 for $\alpha = 1$, which is characteristic of solutions with $\alpha \leq 1$. We see that dS vacuum solutions are always unstable in the imaginary field direction, so these solutions must be stabilized. In Fig. 3.3 we show the scalar potential with $\alpha = 3$, which is characteristic of solutions with $\alpha > 1$. Here, we see that vacuum solutions might fall into an AdS vacuum, which corresponds to the gap region shown in Fig. 3.1. In both cases, the potential is completely flat along the line $y = 0$ corresponding to the dS solution up to the point where $x = 0$ (the potential is not defined at $x \leq 0$).

To address the stability issue, we consider the modified Kähler potential Eq. (3.19), where if we compare it to the general Kähler potential Eq. (3.27), we see that in the real direction the

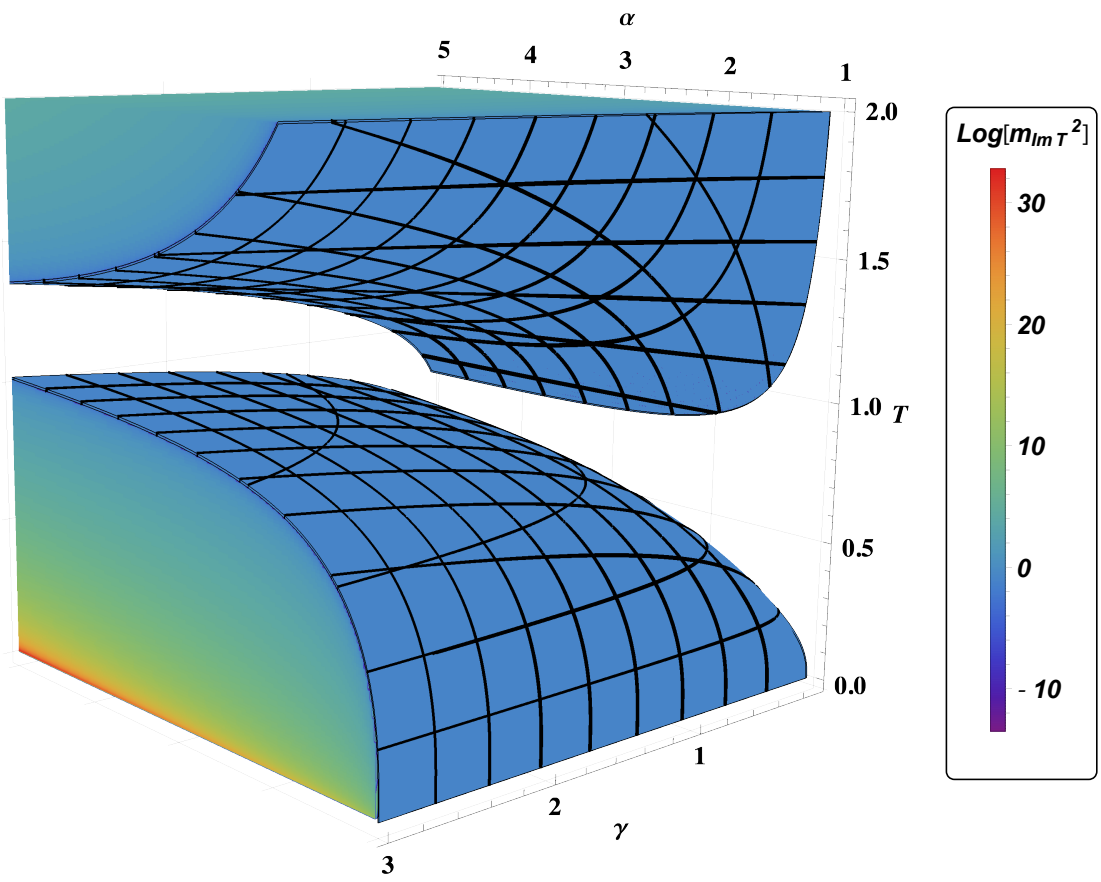

Figure 3.1: Illustration of the value of the expression Eq. (3.34) as a function of (α, γ, T), as shown by the color coding for $\log\left(m^2_{Im\,T}/4\,\lambda_2^2\right)$ on the right-hand side. Reprinted with permission from [13].

argument inside the logarithm remains unchanged, with $\xi = 2T$.

The generalization of the mass squared in Eq. (3.34) is:

$$m^2_{Im\,T} = \frac{4\left[\lambda_1^2(\alpha - 1 + 12\beta\cdot\xi^3)\xi^{-3\sqrt{\alpha}} - 2(\alpha + 1 - 12\beta\cdot\xi^3)\lambda_1\lambda_2 + \lambda_2^2(\alpha - 1 + 12\beta\cdot\xi^3)\xi^{3\sqrt{\alpha}}\right]}{\alpha}\,, \tag{3.35}$$

where it can readily be seen from the numerator of Eq. (3.35) that, by choosing a value of β that is large enough, we can always make the imaginary field direction stable [5]. We plot in Fig. 3.4 and Fig. 3.5 the unstable cases considered previously with $\alpha = 1$ and $\alpha = 3$, which have been each stabilized with the choice $\beta = 2$. Once again, the potential along $y = 0$ is flat.

[5] A similar expression when $\gamma = 1$ can be found in [12].

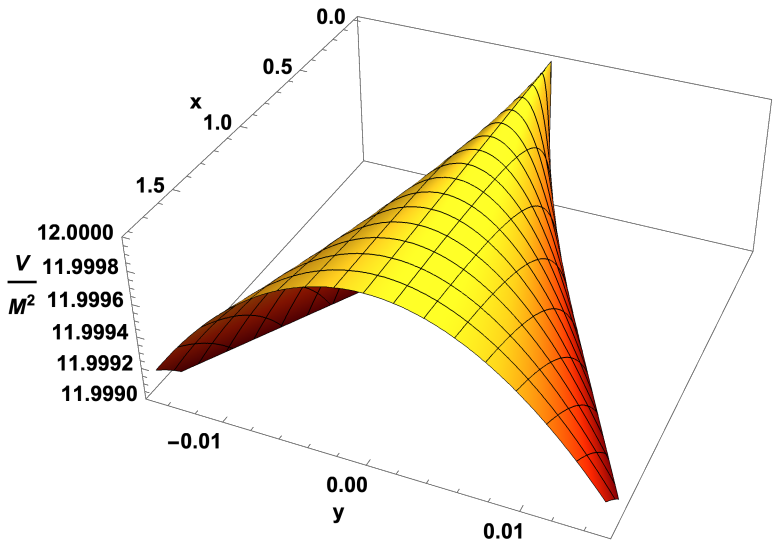

Figure 3.2: The effective scalar potential $V(x, y)$ normalized by M^2 without quartic stabilization terms in the imaginary direction ($\beta = 0$), for the case $\alpha = 1$. Here M is mass of the field along real field direction. Reprinted with permission from [13].

3.3 Multi-Moduli Models

3.3.1 Minkowski Vacuum for Two Moduli

Our next step is to extend this formulation to the two- and multi-moduli cases. As before, we first construct the general Minkowski vacuum solutions and then use Minkowski superpotential pairs to obtain dS/AdS solutions. We begin by considering the following two-field Kähler potential:

$$K \;=\; -3\,\alpha_1 \ln(\mathcal{V}_1) - 3\,\alpha_2 \ln(\mathcal{V}_2)\,. \tag{3.36}$$

For now, we consider $\mathcal{V}_1 = T_1 + \overline{T}_1$ and $\mathcal{V}_2 = T_2 + \overline{T}_2$. Along the real directions, $T_1 = \overline{T}_1$ and $T_2 = \overline{T}_2$, we adopt the following notation:

$$\mathcal{V}_1 \to \xi_1, \qquad \mathcal{V}_2 \to \xi_2\,, \tag{3.37}$$

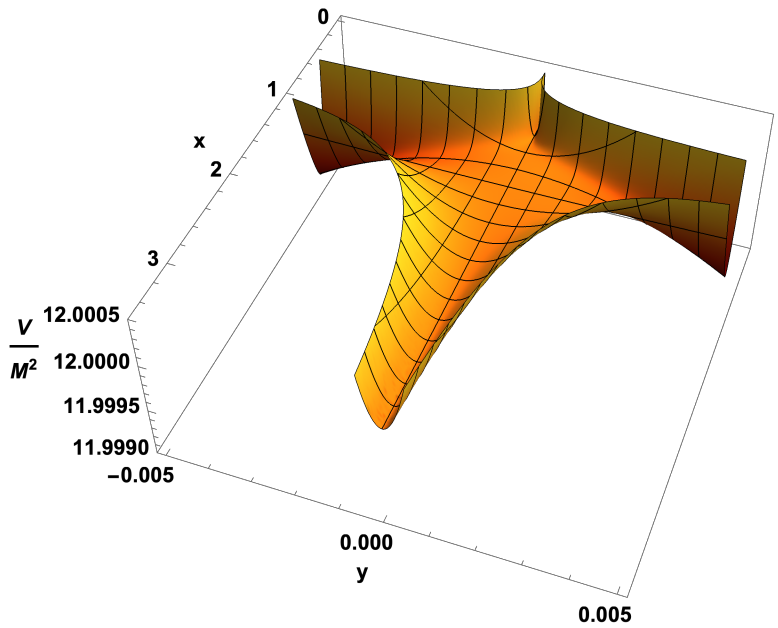

Figure 3.3: The effective scalar potential $V(x, y)$ normalized by M^2 without quartic stabilization terms in the imaginary direction ($\beta = 0$), for the case $\alpha = 3$. Here M is mass of the field along real field direction. Reprinted with permission from [13].

and we choose the following ansatz that yields Minkowski vacuum solutions:

$$W_M = \lambda \cdot \xi_1^{n_1} \cdot \xi_2^{n_2} \,. \tag{3.38}$$

Inserting the superpotential Eq. (3.38) into the expression Eq. (3.5) for the effective scalar potential, we obtain:

$$V = \lambda^2 \cdot \xi_1^{2n_1 - 3\alpha_1} \cdot \xi_2^{2n_2 - 3\alpha_2} \cdot \left(\frac{(2n_1 - 3\alpha_1)^2}{3\alpha_1} + \frac{(2n_2 - 3\alpha_2)^2}{3\alpha_2} - 3 \right) . \tag{3.39}$$

In order to recover Minkowski vacua, we set $V = 0$, which holds when the following expression is satisfied [12]:

$$\frac{(2n_1 - 3\alpha_1)^2}{3\alpha_1} + \frac{(2n_2 - 3\alpha_2)^2}{3\alpha_2} = 3 \,. \tag{3.40}$$

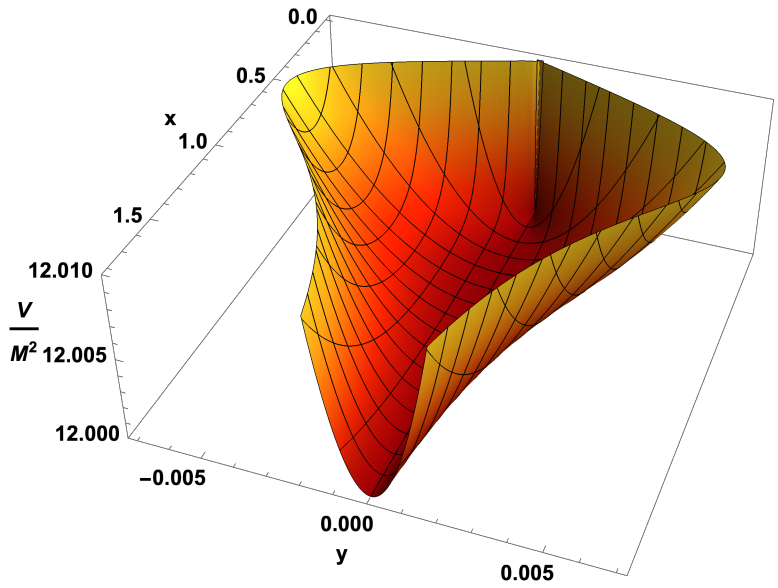

Figure 3.4: The effective scalar potential $V(x, y)$ normalized by M^2 for $\alpha = 1$ now stabilized by quartic terms in the imaginary direction with $\beta = 2$. Here M is mass of the field along real field direction. Reprinted with permission from [13].

For ease of illustration, we introduce the following parametrization:

$$r_1 \equiv \frac{2n_1 - 3\alpha_1}{3\sqrt{\alpha_1}}\,, \qquad r_2 \equiv \frac{2n_2 - 3\alpha_2}{3\sqrt{\alpha_2}}\,, \tag{3.41}$$

in terms of which the general expression Eq. (3.40) becomes:

$$r_1^2 + r_2^2 = 1\,. \tag{3.42}$$

Solving the constraint Eq. (3.40) for n_1 and n_2, we find:

$$n_1 = \frac{3}{2}\left(\alpha_1 \pm \sqrt{1 - \frac{(2n_2 - 3\alpha_2)^2}{9\alpha_2}} \cdot \sqrt{\alpha_1}\right) \quad \text{and} \quad n_2 = \frac{3}{2}\left(\alpha_2 \pm \sqrt{1 - \frac{(2n_1 - 3\alpha_1)^2}{9\alpha_1}} \cdot \sqrt{\alpha_2}\right)\,, \tag{3.43}$$

which can be parametrized using Eq. (3.41):

$$n_1 = \frac{3}{2}\left(\alpha_1 + r_1\sqrt{\alpha_1}\right) \quad \text{and} \quad n_2 = \frac{3}{2}\left(\alpha_2 + r_2\sqrt{\alpha_2}\right)\,, \tag{3.44}$$

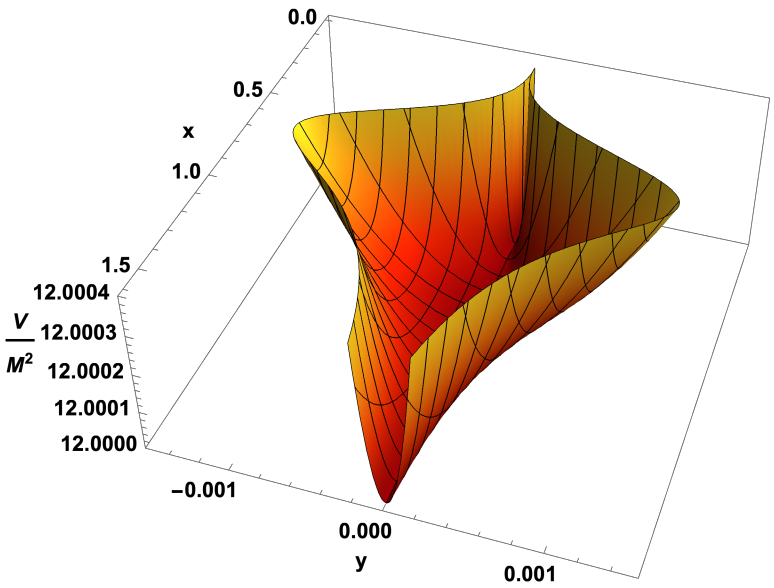

Figure 3.5: The effective scalar potential $V(x, y)$ normalized by M^2 for $\alpha = 3$ now stabilized by quartic terms in the imaginary direction with $\beta = 2$. Here M is mass of the field along real field direction. Reprinted with permission from [13].

where the values of r_1 and r_2 are constrained by expression Eq. (3.42), and must satisfy the condition $r_i \in \{-1, 1\}$. It can already be seen from these equations that the circular parametrization Eq. (3.41) simplifies our expressions significantly, and it will be useful in establishing a geometric connection. We must also satisfy the following inequalities:

$$\alpha_i > 0, \quad \text{with } i = 1, 2\,. \tag{3.45}$$

We see from Eq. (3.44) that we can consider a total of four different sign combinations that yield $V = 0$. The corresponding expressions for the imaginary masses-squared are given by:

$$m^2_{Im\,T_i} = \frac{4\,\lambda^2 \cdot \xi_1^{3r_1\sqrt{\alpha_1}} \cdot \xi_2^{3r_2\sqrt{\alpha_2}}\,(\alpha_i - r_i^2)}{\alpha_i}, \quad \text{with } i = 1, 2\,, \tag{3.46}$$

where stability in the imaginary direction is obtained when the condition $\alpha_i - r_i^2 \geq 0$ is satisfied. If we this combine this inequality with the constraint Eq. (3.42), we obtain another stability condition

in terms of the curvature parameters:

$$\alpha_1 + \alpha_2 \geq 1. \tag{3.47}$$

3.3.2 Minkowski Pair Formulation for Two Moduli

Applying the same approach that we used for the case of a single modulus, we now show how to construct Minkowski pairs for the two-field case and recover dS/AdS vacuum solutions with $V = 12\,\lambda_1\,\lambda_2$ (as in Eq. (3.33)) along the direction where all fields are real. The general dS/AdS vacuum solutions for the two-field case are given by:

$$W_{dS/AdS} = \lambda_1 \cdot \xi_1^{n_1} \cdot \xi_2^{n_2} - \lambda_2 \cdot \xi_1^{\bar{n}_1} \cdot \xi_2^{\bar{n}_2}\,, \tag{3.48}$$

where we define:

$$\bar{n}_1 \equiv \frac{3}{2}\left(\alpha_1 + \bar{r}_1\sqrt{\alpha_1}\right) \quad \text{and} \quad \bar{n}_2 \equiv \frac{3}{2}\left(\alpha_2 + \bar{r}_2\sqrt{\alpha_2}\right)\,, \tag{3.49}$$

with the expressions for $n_{1,2}$ being given by Eq. (3.44) and $\bar{r}_i = -r_i$. We note that the powers Eq. (3.49) describe the antipode of a point lying on the surface of a circle described by the coordinates (r_1, r_2), and we discuss the geometric interpretation of our models in the next Section.

The scalar masses recovered from the dS/AdS superpotential Eq. (3.48) have complicated expressions that we do not list here. However, we note that we can always modify the initial Kähler potential Eq. (3.36) by including higher-order corrections in the imaginary direction:

$$K = -3\,\alpha_1 \ln\left(T_1 + \overline{T}_1 + \beta_1\left(T_1 - \overline{T}_1\right)^4\right) - 3\,\alpha_2 \ln\left(T_2 + \overline{T}_2 + \beta_2\left(T_2 - \overline{T}_2\right)^4\right), \tag{3.50}$$

where these quartic terms easily remedy the stability problems [12]. If we compare it to the general two-field Kähler potential in Eq. (3.36), along the real directions, $T_1 = \overline{T}_1$ and $T_2 = \overline{T}_2$, we recover $\xi_1 = 2T_1$ and $\xi_2 = 2T_2$. In the next Section we extend this formulation to the N-field case.

3.3.3 Minkowski Pair Formulation for Multiple Moduli

We now show how to generalize our formulation and construct successfully the Minkowski pair superpotential for cases with $N > 2$ moduli. We first introduce the following Kähler potential:

$$K = -3\sum_{i=1}^{N} \alpha_i \ln\left(\mathcal{V}_i\right) \,, \tag{3.51}$$

where $\mathcal{V}_i = T_i + \overline{T}_i$. Next, we impose the condition that all our fields are real, therefore $T_i = \overline{T}_i$, which leads to:

$$\mathcal{V}_i \longrightarrow \xi_i, \quad \text{for } i = 1, 2, ..., N \,. \tag{3.52}$$

Minkowski vacuum solutions are obtained with the choice:

$$W_M = \lambda \cdot \prod_{i=1}^{N} \xi_i^{n_i} \tag{3.53}$$

in the general N-field case. Inserting the superpotential Eq. (3.53) into Eq. (3.5), we find:

$$V = \lambda^2 \cdot \prod_{i=1}^{N} \xi_i^{2n_i - 3\alpha_i} \cdot \left(\sum_{i=1}^{N} \frac{(2n_i - 3\alpha_i)^2}{3\alpha_i} - 3 \right) \,, \tag{3.54}$$

and it can be seen from Eq. (3.54) that in order to obtain Minkowski vacuum solutions: $V = 0$, we must satisfy the constraint:

$$\sum_{i=1}^{N} \frac{(2n_i - 3\alpha_i)^2}{3\alpha_i} = 3 \,. \tag{3.55}$$

Once again, we introduce the following parametrization:

$$r_i \equiv \frac{2n_i - 3\alpha_i}{3\sqrt{\alpha_i}}, \quad \text{for } i = 1, 2, ..., N \,, \tag{3.56}$$

and combining the Eq. (3.55) and Eq. (3.56) we obtain:

$$\sum_{i=1}^{N} r_i^2 = 1 \,. \tag{3.57}$$

Therefore, Eq. (3.57) parametrizes the N-field Minkowski solutions as lying on the surface of an $(N-1)$-sphere.

Solving Eq. (3.56) for n_i, we obtain:

$$n_i = \frac{3}{2}\left(\alpha_i + r_i\sqrt{\alpha_i}\right), \quad \text{for } i = 1, 2, ..., N\,, \tag{3.58}$$

where $r_i \in \{-1, 1\}$ and $\alpha_i > 0$. For the N-moduli case, we obtain the following expression for the scalar masses-squared in the imaginary directions:

$$m^2_{Im\,T_i} = \frac{4\lambda^2\left(\alpha_i - r_i^2\right)\prod_{i=1}^{N}\xi_i^{-3r_i\sqrt{\alpha_i}}}{\alpha_i}, \quad \text{with } i = 1, 2, ..., N\,. \tag{3.59}$$

To obtain a stable solution in the imaginary direction, we must satisfy the condition $\alpha_i - r_i^2 \geq 0$. If we use the constraint of the $(N-1)$-sphere Eq. (3.57), we obtain the following stability condition:

$$\sum_{i=1}^{N}\alpha_i \geq 1. \tag{3.60}$$

Following the procedure described previously, we combine a pair of Minkowski solutions Eq. (3.53) and introduce the following dS/AdS superpotential:

$$W_{dS/AdS} = \lambda_1 \cdot \prod_{i=1}^{N}\xi_i^{n_i} - \lambda_2 \cdot \prod_{i=1}^{N}\xi_i^{\bar{n}_i}\,, \tag{3.61}$$

where $\bar{n}_i = \frac{3}{2}\left(\alpha_i + \bar{r}_i\sqrt{\alpha_i}\right)$, with $\bar{r}_i = -r_i$. This superpotential form also yields the familiar dS/AdS vacuum result $V = 12\,\lambda_1\,\lambda_2$.

It proves difficult to perform a detailed stability analysis for N-moduli models, because this would involve finding the eigenvalues of an $N \times N$ matrix. Nevertheless, one can always introduce higher-order corrections in the Kähler potential Eq. (3.51):

$$K = -3\sum_{i=1}^{N}\alpha_i \ln\left(T_i + \overline{T}_i + \beta_i\left(T_i - \overline{T}_i\right)^4\right), \tag{3.62}$$

where the quartic terms stabilize the imaginary directions [12]. If we compare the multi-moduli Kähler potential Eq. (3.51) with Eq. (3.62), we see that along the real directions, $T_i = \overline{T}_i$, and we recover $\xi_i = 2T_i$.

3.3.4 Geometric Interpretation

We now discuss the geometric interpretation of this Minkowski pair formulation. From Eq. (3.55-3.57) it is clear that our parametrization describes Minkowski superpotential solutions Eq. (3.53) that lie on the surface of an $(N-1)$-sphere that is embedded in Euclidean N-space. We first return to the two-moduli case, in which the Eq. (3.57) reduces to Eq. (3.42), and all Minkowski solutions lie on a circle embedded in 2-dimensional space. We define the radius vector of points on a circle r by:

$$r \;=\; (r_1, r_2)\,, \qquad \text{with } r_1^2 + r_2^2 = 1. \tag{3.63}$$

As expected, Eq. (3.63) includes 4 possible sign combinations corresponding to different quadrants of a circle. To construct successfully a Minkowski pair superpotential that yields a dS/AdS vacuum solution, we must combine any chosen point on the circle with its antipodal point, given by the vector:

$$\bar{r} \;=\; -r = -\left(r_1, r_2\right)\,. \tag{3.64}$$

In this way, we can construct an infinite number of distinct Minkowski superpotential pairs by considering different point/antipode combinations lying on the surface of a circle. The Minkowski pair construction on a circle is illustrated in Fig. 3.6. For any value of $\alpha > 0$, Eq. (3.48) will yield a dS or AdS solution so long as $n_i = \frac{3}{2}\left(\alpha_i + r_i\sqrt{\alpha}_i\right)$ and $\bar{n}_i = \frac{3}{2}\left(\alpha_i + \bar{r}_i\sqrt{\alpha}_i\right)$.

We can readily generalize this framework to the N-moduli case, in which we define the radius vector r to lie on the surface of an $(N-1)$-sphere, and it is expressed as:

$$r = (r_1, r_2, ..., r_N)\,, \qquad \text{with } \sum_{i=1}^{N} r_i^2 = 1\,, \tag{3.65}$$

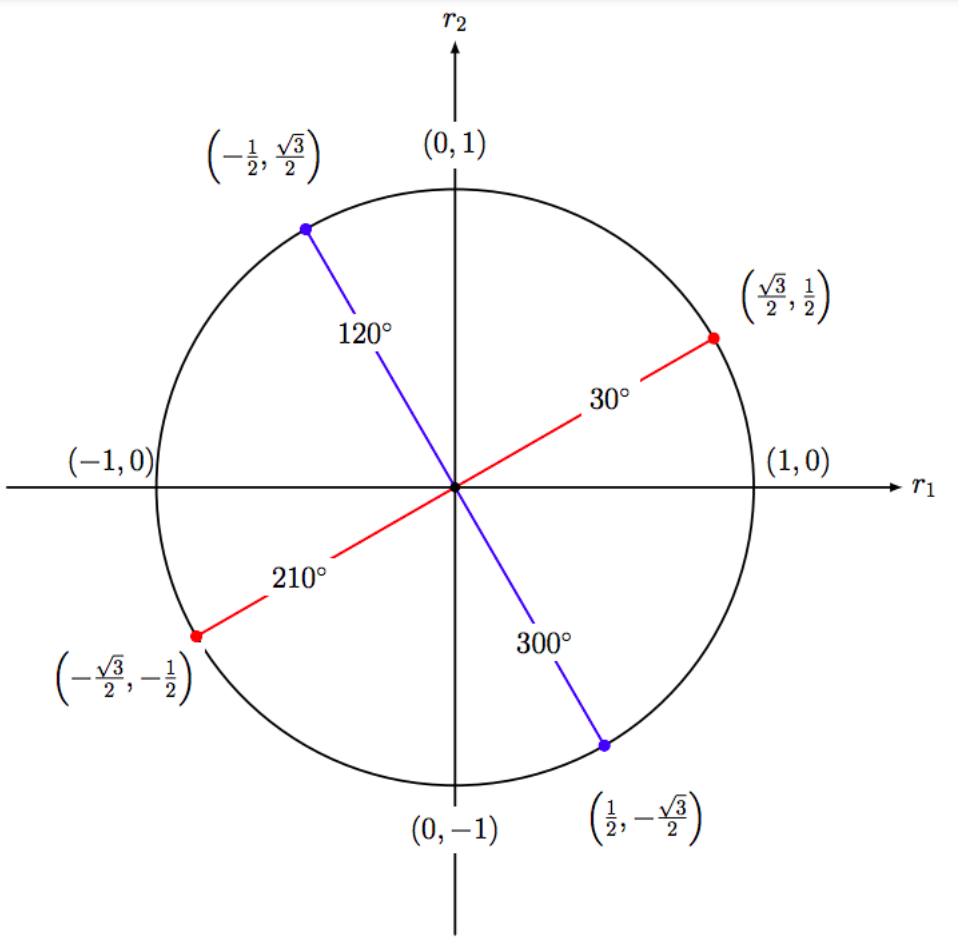

Figure 3.6: Depiction of Minkowski pairs on a circle. The circle is split into four quadrants and two distinct Minkowski pairs are shown lying in different quadrants. The red dots show a Minkowski pair solution $r = (\sqrt{3}/2, 1/2)$ and $\bar{r} = (-\sqrt{3}/2, -1/2)$, which lies in the first and third quadrants of the circle, while the blue dots show a Minkowski pair solution $r = (-1/2, \sqrt{3}/2)$ and $\bar{r} = (1/2, -\sqrt{3}/2)$, which lies in the second and fourth quadrants of the circle. Reprinted with permission from [13].

while the antipodal vector $\bar{r}$ is given by:

$$\bar{r} = -\left(r_1, r_2, ..., r_N\right) \ . \tag{3.66}$$

As an illustration, we consider the three-field case: $N = 3$. In this case, the Minkowski solutions lie anywhere on the surface of the unit sphere. dS and AdS solutions can be obtained from any point on the sphere, by combining it with this antipodal point with $r_i \to -r_i$. In Fig. 3.7 we

show an example where four different Minkowski vacuum solutions are combined into 2 distinct Minkowski pairs lying on the surface of a sphere.

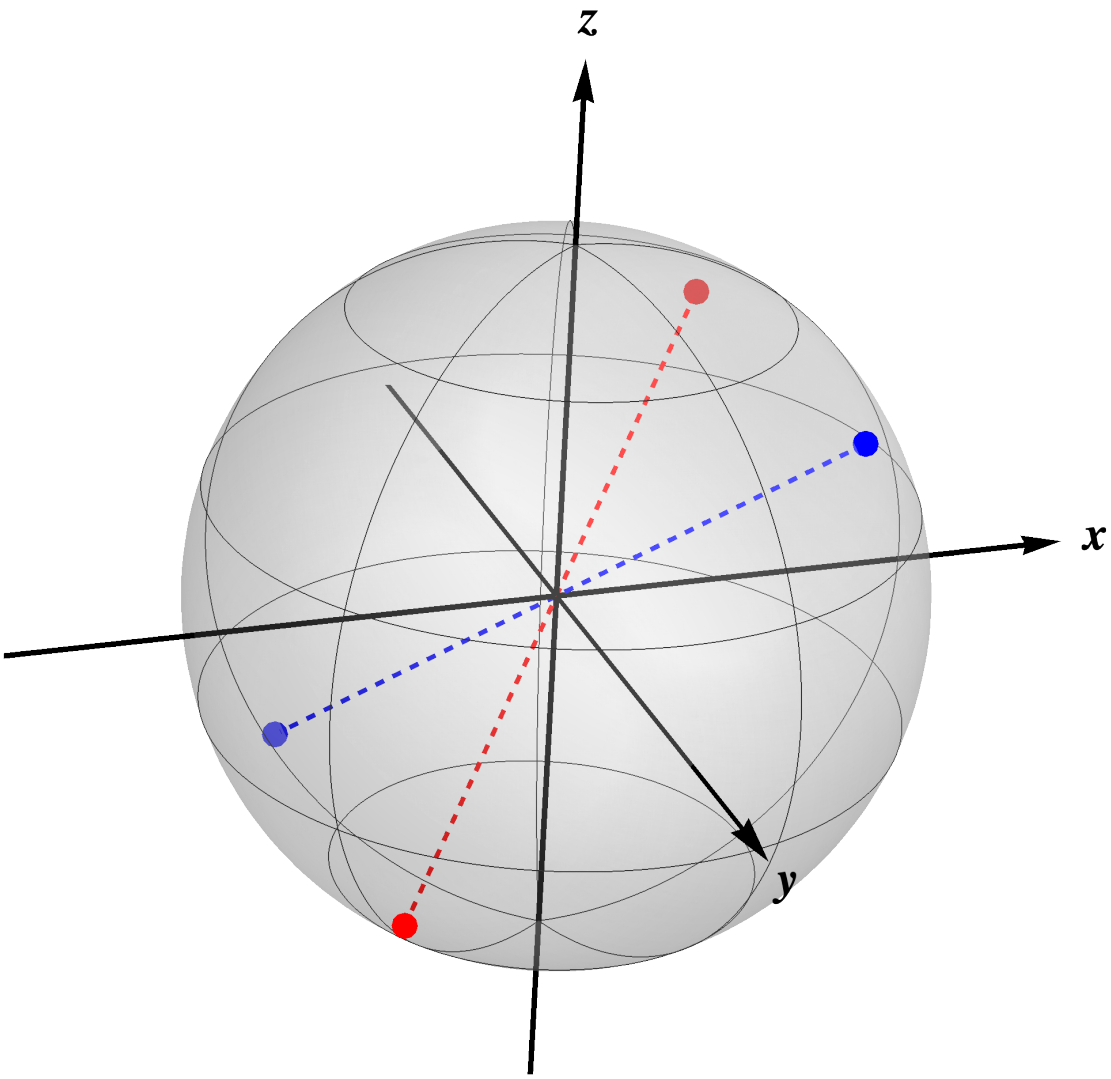

Figure 3.7: Illustration of Minkowski pairs on the surface of a sphere. The sphere is split into eight octants and two distinct Minkowski pairs lying in different octants are shown. The red dots represent a Minkowski pair solution $r = (1/\sqrt{3}, -1/\sqrt{3}, 1/\sqrt{3})$ and $\bar{r} = (-1/\sqrt{3}, 1/\sqrt{3}, -1/\sqrt{3})$, which lies in the fourth and sixth octants of the sphere, while the blue dots represent a Minkowski pair solution $r = (1/\sqrt{3}, 1/\sqrt{3}, 1/\sqrt{3})$ and $\bar{r} = (-1/\sqrt{3}, -1/\sqrt{3}, -1/\sqrt{3})$, which lies in the first and seventh octants of the sphere. Reprinted with permission from [13].

We have seen how all Minkowski pair solutions lie on the surface of an $(N-1)$-sphere of unit

radius, and recall the general expressions for the corresponding powers, n_i and $\bar{n}_i$ of ξ given earlier: We show in Fig. 3.8 Minkowski pair solutions for these powers as functions of $|r_i|$ and α_i. The lower yellow sheet illustrates the possible choices for n_i, while the upper blue sheet illustrates the possible choices for $\bar{n}_i$. If we are only concerned with Minkowski solutions, we can freely choose any point lying on either the upper or lower sheet, which leads to $V = 0$. In order to construct successfully a Minkowski pair, we need to combine our chosen point with the corresponding point on the opposite sheet, which will yield the dS/AdS solution $V = 12\,\lambda_1\,\lambda_2$.

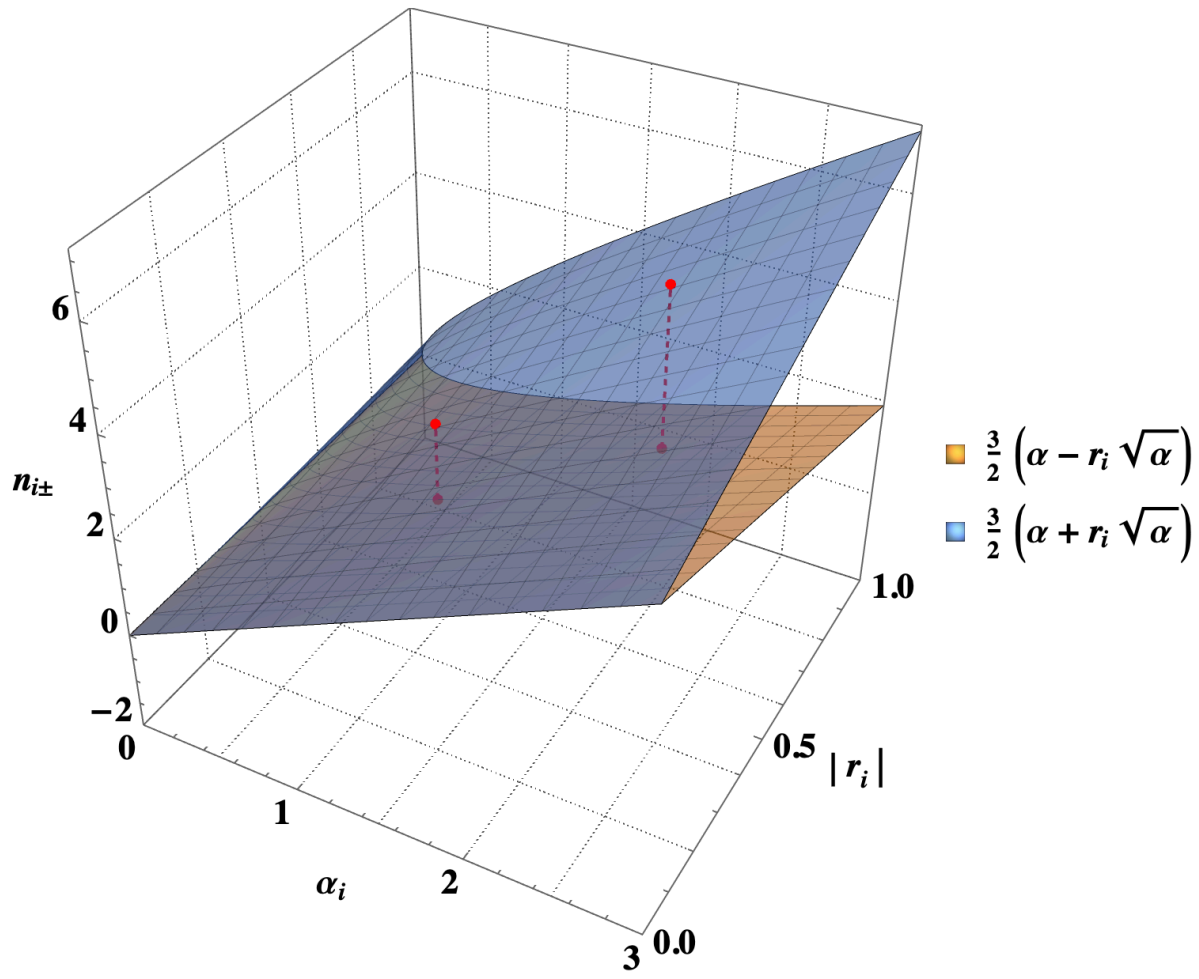

Figure 3.8: Illustration of Minkowski pair formulation on the n_i (yellow) and $\bar{n}_i$ (blue) sheets. The Minkowski pairs are depicted by red dots and their coordinates are given by $\left(1, \frac{1}{2}, \frac{3}{4}\right)$ with $\left(1, \frac{1}{2}, \frac{9}{4}\right)$ and $\left(2, \frac{3}{4}, 3 - \frac{9}{8}\sqrt{2}\right)$ with $\left(2, \frac{3}{4}, 3 + \frac{9}{8}\sqrt{2}\right)$. Reprinted with permission from [13].

Having established successfully a geometric connection between unique vacuum solutions, in the remaining sections we show that identical patterns emerge for Kähler potential forms with untwisted and twisted matter fields.

3.4 Minkowski Pairs with Matter Fields

3.4.1 The Untwisted Case

In this Section, we extend our formulation to no-scale models with untwisted matter fields. We begin by considering the following Kähler potential, which parametrizes a non-compact $\frac{SU(2,1)}{SU(2)\times U(1)}$ coset space:

$$K \;=\; -3\,\alpha \ln\left(T+\overline{T}-\frac{\phi\bar{\phi}}{3}\right)\,, \tag{3.67}$$

where α is a curvature parameter, T can be interpreted as a volume modulus, and ϕ is a matter field. Moreover, we impose the conditions $T=\overline{T}$ and $\phi=\bar{\phi}$ by fixing the VEVs of the imaginary components of the fields to zero, along the lines discussed above. Clearly Eq. (3.67) can be written in the form of Eq. (3.27) with $\mathcal{V}$ set equal to the argument of the $\log$ in Eq. (3.67), $\mathcal{V}=T+\overline{T}-\frac{\phi\bar{\phi}}{3}$.

Once again, when we restrict to real fields, and in this case set $T=\overline{T}$ and $\phi=\bar{\phi}$ we obtain:

$$\mathcal{V}\longrightarrow\xi, \qquad \text{with} \qquad \xi=2T-\frac{\phi^2}{3}\,. \tag{3.68}$$

We then consider the following form of superpotential:

$$W_M \;=\; \lambda\cdot\xi^n\,, \tag{3.69}$$

which leads to the following effective scalar potential:

$$V=\lambda^2\,\xi^{2n-3\alpha}\cdot\left(\frac{(2n-3\alpha)^2}{3\alpha}-3\right)\,. \tag{3.70}$$

To obtain a Minkowski vacuum: $V=0$, we solve the constraint for n, and recover the familiar result given in Eq. (3.8) for the case with a single modulus. Using the superpotential in Eq. (3.69),

we find the following scalar masses-squared for the imaginary components of the fields T and ϕ:

$$m^2_{Im\,T} = \frac{4\lambda^2(\alpha-1)\xi^{\pm 3\sqrt{\alpha}}}{\alpha}, \quad m^2_{Im\,\phi} = \frac{4\lambda^2(\sqrt{\alpha}\pm 1)\xi^{\pm 3\sqrt{\alpha}}}{\sqrt{\alpha}}\,, \tag{3.71}$$

whereas, as anticipated, the masses-squared of the real components are $m^2_{Re\,T} = 0$ and $m^2_{Re\,\phi} = 0$. It can be seen from Eqs. (3.71) that stability in the imaginary directions for both fields requires that the inequalities $\alpha \geq 1$.

To construct the $\frac{SU(2,1)}{SU(2)\times U(1)}$ Minkowski pair formulation, we follow the previous discussion and use the same superpotential as in Eq. (3.32)

$$W_{dS/AdS} = \lambda_1 \cdot \xi^{n_-} - \lambda_2 \cdot \xi^{n_+}\,. \tag{3.72}$$

Doing so, we recover dS/AdS vacuum solutions given by Eq. (3.33). In this case, the masses-squared for the imaginary field components are given by:

$$m^2_{Im\,T} = \frac{4\left(\lambda_1^2(\alpha-1)\xi^{-3\sqrt{\alpha}} - 2(\alpha+1)\lambda_1\lambda_2 + \lambda_2^2(\alpha-1)\xi^{3\sqrt{\alpha}}\right)}{\alpha} \tag{3.73}$$

and

$$m^2_{Im\,\phi} = 4\left(\frac{\lambda_1^2(\sqrt{\alpha}-1)\xi^{-3\sqrt{\alpha}}}{\sqrt{\alpha}} + 4\lambda_1\lambda_2 + \frac{\lambda_2^2(\sqrt{\alpha}+1)\xi^{3\sqrt{\alpha}}}{\sqrt{\alpha}}\right). \tag{3.74}$$

We do not discuss here the stabilization of these components, but we can always include quartic stabilization terms in the Kähler potential Eq. (3.67), as discussed previously.

Having established the principles in the case of the $\frac{SU(2,1)}{SU(2)\times U(1)}$ Kähler potential with an untwisted matter field ϕ, we can generalize our formulation to no-scale models that parametrize a non-compact $\frac{SU(N,1)}{SU(N)\times U(1)}$ coset manifold. Following the same recipe considered in previous sections, we start with the Kähler potential Eq. (3.27), and we define the argument inside the logarithm as:

$$\mathcal{V} \equiv T + \overline{T} - \sum_{j=1}^{N-1} \frac{|\phi_j|^2}{3}\,. \tag{3.75}$$

Furthermore, we fix the VEVs of the imaginary fields to zero, so that $T = \overline{T}$ and $\phi_j = \bar{\phi}_j$. Using the same notation:

$$\mathcal{V} \longrightarrow \xi, \text{ when } T = \overline{T} \text{ and } \phi_j = \bar{\phi}_j \,, \tag{3.76}$$

the argument inside the logarithm in the Kähler potential becomes

$$\xi = 2T - \sum_{j=1}^{N-1} \frac{|\phi_j|^2}{3} \,. \tag{3.77}$$

With this definition of ξ, Minkowski vacuum solutions are found for the same choice of superpotential given in Eq. (3.69). The masses-squared of the imaginary components, with $m^2_{Im\,T}$ and $m^2_{Im\,\phi_j}$ are given by Eq. (3.71).

At this point, it should not be surprising that by combining two distinct Minkowski solutions we can form a Minkowski superpotential pair given by Eq. (3.72). This dS/AdS superpotential yields identical scalar masses-squared for the imaginary components, with $m^2_{Im\,T}$ given by Eq. (3.73) and $m^2_{Im\,\phi_j}$ given by Eq. (3.74).

Finally, we can also extend our formulation to more complicated Kähler potentials that take the form $K = \sum_i K_i$, where each K_i is of no-scale type and given by:

$$K = -3 \prod_{i=1}^{M} \alpha_i \ln(\mathcal{V}_i), \quad \text{with } \mathcal{V}_i = T_i + \overline{T}_i - \sum_{j=1}^{N-1} \frac{|\phi_{ij}|^2}{3} \,. \tag{3.78}$$

We again assume that $T_i = \bar{T}_i$ and $\phi_{ij} = \bar{\phi}_{ij}$, which leads to:

$$\mathcal{V}_i \longrightarrow \xi_i, \text{ when } T_i = \bar{T}_i \text{ and } \phi_{ij} = \bar{\phi}_{ij} \,. \tag{3.79}$$

Thus, we obtain the following Minkowski pair superpotential:

$$W_{dS/AdS} = \lambda_1 \cdot \prod_{i=1}^{M} \xi_i^{n_i} - \lambda_2 \cdot \prod_{i=1}^{M} \xi_i^{\bar{n}_i}, \quad \text{with } V = 12\,\lambda_1\,\lambda_2 \,, \tag{3.80}$$

which coincides with the multi-moduli case considered previously.

3.4.2 The Twisted Case

An analogous Minkowski pair formulation can also be considered in the case of twisted matter fields. We consider the corresponding Kähler potential:

$$K \;=\; -3\,\alpha\,\ln\left(T+\overline{T}\right)+\varphi\bar{\varphi}\,, \tag{3.81}$$

where we introduce the notation φ for twisted matter fields. To this end, we first find a relatively simple superpotential form that yields Minkowski solutions, and consider the following Ansatz:

$$W_M = \lambda\cdot(2T)^n\cdot e^{-\varphi^2/2}\,. \tag{3.82}$$

Combining it with the effective scalar potential in Eq. (3.5), and setting $T=\overline{T}$ and $\varphi=\bar{\varphi}$ by fixing the VEVs of the imaginary components of the fields to zero, we obtain:

$$V=\lambda^2\cdot(2T)^{2n-3\alpha}\cdot\left(\frac{(2n-3\alpha)^2}{3\alpha}-3\right)\,. \tag{3.83}$$

From the form of the scalar potential, we see that it does not depend on $Re\,\varphi$. To obtain a Minkowski vacuum solution, we find the same solutions found in Eq. (3.8) for n. This yields the following scalar masses-squared for the imaginary components:

$$m^2_{Im\,T} \;=\; \frac{4\lambda^2(\alpha-1)}{\alpha}\cdot(2T)^{\pm3\sqrt{\alpha}} \tag{3.84}$$

and

$$m^2_{Im\,\varphi} \;=\; 4\,\lambda^2\,(2T)^{\pm3\sqrt{\alpha}}\,. \tag{3.85}$$

We can see from Eq. (3.84) and Eq. (3.85) that $Im\,\varphi$ is always stable, and that $Im\,T$ is stable when $\alpha\geq1$.

Similarly, we also consider the following Ansatz:

$$W_M = \lambda \cdot (2T)^n \cdot e^{+\varphi^2/2} \,. \tag{3.86}$$

If we combine this with Eq. (3.5), and set $T = \overline{T}$ and $\varphi = -\bar{\varphi}$, we obtain the same effective scalar potential Eq. (3.83) with solutions for n given by Eq. (3.8). In this case, the scalar potential does not depend on $Im\,\varphi$, and the scalar masses-squared are given by Eq. (3.84) and Eq. (3.85) [6]. Therefore, there are two ways to construct Minkowski vacuum solutions with twisted matter fields that do not depend on either the real or imaginary components of φ.

Next, we construct the dS/AdS superpotential by combining two distinct Minkowski solutions:

$$W_{dS/AdS} = \left(\lambda_1 \cdot (2T)^{n_-} - \lambda_2 \cdot (2T)^{n_+}\right) \cdot e^{-\varphi^2/2} \,, \tag{3.87}$$

where we choose a Minkowski pair construction which does not depend on $Re\,\varphi$, and, if we assume that $T = \overline{T}$ and $\varphi = \bar{\varphi}$, the effective scalar potential Eq. (3.5) is given by Eq. (3.33) once again. In the case of the superpotential Eq. (3.87), the scalar masses-squared of the imaginary field components are:

$$m^2_{Im\,T} \;=\; \frac{4\left(\lambda_1^2(\alpha-1)\,(2T)^{-3\sqrt{\alpha}} - 2(\alpha+1)\lambda_1\lambda_2 + \lambda_2^2(\alpha-1)\,(2T)^{3\sqrt{\alpha}}\right)}{\alpha} \tag{3.88}$$

and

$$m^2_{Im\,\varphi} \;=\; 4\left(\lambda_1^2(2T)^{-3\sqrt{\alpha}} + 4\lambda_1\,\lambda_2 + \lambda_2^2(2T)^{3\sqrt{\alpha}}\right) \,. \tag{3.89}$$

It is important to note that for de Sitter solutions, while $m^2_{Im\,\varphi}$ is always positive, $m^2_{Im\,T}$ is not and may require quartic stabilization terms in the imaginary direction for the field T.

[6] It is important to note that in this case the effective scalar potential has curvature in the real direction and the scalar mass-squared expression Eq. (3.85) becomes $m^2_{Re\,\varphi}$.

Analogously, one can also consider the following dS/AdS superpotential form:

$$W_{dS/AdS} = \left(\lambda_1 \cdot (2T)^{n_-} - \lambda_2 \cdot (2T)^{n_+}\right) \cdot e^{+\varphi^2/2}\,, \tag{3.90}$$

where, after setting $T = \overline{T}$ and $\phi = -\bar{\phi}$, we obtain the dS/AdS scalar potential $V = 12\,\lambda_1\lambda_2$, with the scalar masses-squared given by Eq. (3.88) and Eq. (3.89).

This analysis with a single twisted matter field can be generalized to include multiple fields. We consider the following Kähler potential form:

$$K \;=\; -3\,\alpha\,\ln(\mathcal{V}) + \sum_{j=1}^{N} |\varphi_j^2|\,. \tag{3.91}$$

In this case, all of the previous results hold after the simple substitution of $\varphi^2 \to \sum \varphi_j^2$.

Another possible generalization is to consider Kähler potentials of the form $K = \sum_i K_i + \sum_j |\varphi_j|^2$, where each K_i is of no-scale type:

$$K \;=\; -\,3\sum_{i=1}^{M} \alpha_i \ln(\mathcal{V}_i) + \sum_{j=1}^{N} |\varphi_j|^2, \quad \text{with } \mathcal{V}_i = T_i + \overline{T}_i\,. \tag{3.92}$$

As before, we assume that:

$$\mathcal{V}_i \longrightarrow \xi_i, \text{ when } T_i = \overline{T}_i. \tag{3.93}$$

In this case, with a superpotential of the form

$$W_M = \lambda \cdot \prod_{i=1}^{M} \xi_i^{n_i} \cdot \exp\left(-\frac{1}{2}\sum_{j=1}^{N} \omega_j \varphi_j^2\right), \tag{3.94}$$

where ω_j can take a value of either $+1$ or -1, we get a Minkowski solution $V = 0$ after setting $T_i = \overline{T}_i$ and $\varphi_j = \omega_j \overline{\varphi}_j$. Similarly, we can obtain dS/AdS solutions $V = 12\,\lambda_1\,\lambda_2$ along the

direction $T_i = \overline{T}_i$, $\varphi_j = \omega_j \overline{\varphi}_j$ from the superpotential:

$$W_{dS/AdS} = \left(\lambda_1 \cdot \prod_{i=1}^{M} \xi_i^{n_i} - \lambda_2 \cdot \prod_{i=1}^{M} \xi_i^{\bar{n}_i} \right) \cdot \exp\left(-\frac{1}{2} \sum_{j=1}^{N} \omega_j \varphi_j^2 \right). \tag{3.95}$$

3.4.3 The Combined Case

We note finally that one can consider more complicated cases combining twisted and untwisted matter fields by following the principles discussed earlier in this Section. The only difference is that one needs to modify the Kähler potential in Eq. (3.92) and introduce untwisted matter fields ϕ_{ik}:

$$K \;=\; -3 \sum_{i=1}^{M} \alpha_i \ln(\mathcal{V}_i) + \sum_{j=1}^{N} |\varphi_j|^2, \quad \text{with } \mathcal{V}_i = T_i + \overline{T}_i + \sum_{k=1}^{P-1} |\phi_{ik}|^2 \,, \tag{3.96}$$

If we assume that all our fields are fixed to be real, this leads to:

$$\mathcal{V}_i \longrightarrow \xi_i, \text{ when } T_i = \overline{T}_i, \; \phi_{ik} = \bar{\phi}_{ik}, \text{ and } \varphi_j = \bar{\varphi}_j \,, \tag{3.97}$$

and for this case Minkowski solutions are given by superpotential Eq. (3.94) and dS/AdS solutions are given by Eq. (3.95).

3.5 Applications to Inflationary Models

3.5.1 Inflation with an Untwisted Matter Field

We now indicate briefly how to construct inflationary models in this framework [39, 40]. For simplicity, we use a non-compact $\frac{SU(2,1)}{SU(2)\times U(1)}$ Kähler potential Eq. (3.67), and we associate the matter field ϕ with the inflaton. If we set $\alpha = 1$, the Kähler potential Eq. (3.67) becomes:

$$K \;=\; -3 \ln\left(T + \overline{T} - \frac{\phi\bar{\phi}}{3} \right). \tag{3.98}$$

Next, we introduce a unified superpotential that combines the Minkowski pair superpotential W_{dS} with an inflationary superpotential $W_I = f(\phi)$:

$$W = W_I + W_{dS} = Mf(\phi) + \lambda_1 - \lambda_2 \left(2T - \frac{\phi^2}{3}\right)^3 . \tag{3.99}$$

We also require that supersymmetry is broken at the minimum through the Minkowski pair superpotential W_{dS} instead of the inflationary superpotential W_I. Therefore, we impose the conditions that $f(0) = f'(0) = 0$. Again, we assume that $T = \overline{T}$ and $\phi = \overline{\phi}$, and the superpotential Eq. (3.99) then yields the following effective scalar potential:

$$V \;=\; 12\lambda_1\,\lambda_2 + 12\lambda_2 M f(\phi) + \frac{M^2 f'(\phi)^2}{\left(2T - \frac{\phi^2}{3}\right)^2}\,, \tag{3.100}$$

where we can safely neglect the mixing terms between λ_2 and M, leading to the approximation:

$$V \;\approx\; 12\lambda_1\,\lambda_2 + \frac{M^2 f'(\phi)^2}{\left(2T - \frac{\phi^2}{3}\right)^2}\,. \tag{3.101}$$

Supersymmetry is broken by an F-term, which is given by:

$$\sum_{i=1}^{2} |F_i|^2 = F_T^2 = (\lambda_1 + \lambda_2)^2\,, \text{ with } m_{3/2} = \lambda_1 - \lambda_2\,. \tag{3.102}$$

3.5.2 Inflation with a Twisted Matter Field

Following the same approach, we now show how to construct viable inflationary models with a twisted inflaton field. We use a non-compact $\frac{SU(1,1)}{U(1)} \times U(1)$ Kähler potential form Eq. (3.81), and we associate the matter field φ with the inflaton. We set $\alpha = 1$, and Eq. (3.81) reduces to:

$$K \;=\; -3\ln\left(T + \overline{T}\right) + \varphi\overline{\varphi}\,. \tag{3.103}$$

Next, we introduce the following unified superpotential form [7]:

$$W = W_I + W_{dS} = \left(M\, f(\varphi) + \lambda_1 - \lambda_2 \left(2T\right)^3 \right) \cdot e^{-\varphi^2/2} \,, \tag{3.104}$$

where the inflationary superpotential is given by $W_I = M\, f(\varphi) \cdot e^{-\varphi^2/2}$. We again require supersymmetry to be broken through the Minkowski pair superpotential W_{dS}, and we impose the conditions that at the minimum we must have $f(0) = f'(0) = 0$. The superpotential form Eq. (3.104) leads to the following effective scalar potential:

$$V = 12\lambda_1\lambda_2 + 12\lambda_2 M f(\varphi) + \frac{M^2 f'(\varphi)^2}{8T^3} \,. \tag{3.105}$$

If we neglect the mixing terms between λ_2 and M, and fix $\langle T \rangle = \frac{1}{2}$, we can approximate:

$$V \approx 12\lambda_1\lambda_2 + M^2 f'(\varphi)^2 \,, \tag{3.106}$$

and supersymmetry breaking is characterized by the same expression given in Eq. (3.102). In order to construct a Starobinsky-like inflationary potential that is a function of the field φ, we use the following canonical field redefinition:

$$\varphi = \frac{x + iy}{\sqrt{2}} \,, \tag{3.107}$$

and we assume that $\varphi = \overline{\varphi} = \frac{x}{\sqrt{2}}$. We then introduce the following inflationary superpotential form:

$$W_I = \frac{3}{4} M \left(\frac{2\varphi}{\sqrt{3}} + e^{-\frac{2\varphi}{\sqrt{3}}} - 1 \right) e^{-\varphi^2/2} \,, \tag{3.108}$$

[7] Similarly, we can consider a unified superpotential form with W_{dS} given by Eq. (3.90). In this case, inflation will be driven by $Im\,\varphi$.

and assume that $\varphi = \overline{\varphi} = \frac{x}{\sqrt{2}}$ and $T = \overline{T} = 1/2$, which yields the Starobinsky inflationary potential with a positive cosmological constant at the minimum:

$$V = 12\lambda_1\lambda_2 + 3\lambda_2 M\left(\sqrt{6}x + 3e^{-\sqrt{\frac{2}{3}}x} - 3\right) + \frac{3}{4}M^2\left(1 - e^{-\sqrt{\frac{2}{3}}x}\right)^2, \tag{3.109}$$

or if we neglect the mixing terms between λ_2 and M, we obtain:

$$V \approx 12\,\lambda_1\lambda_2 + \frac{3}{4}M^2\left(1 - e^{-\sqrt{\frac{2}{3}}x}\right)^2. \tag{3.110}$$

3.6 Summary

We have exhibited in this chapter the unique choice of superpotential leading to a Minkowski vacuum in a single-field no-scale supergravity model, and also shown how to construct dS/AdS solutions using pairs of these single-field Minkowski superpotentials. We have then extended these constructions to two- and multifield no-scale supergravity models, providing also a geometrical interpretation of the dS/AdS solutions in terms of combinations of superpotentials that are functions of fields at antipodal points on hyperspheres. As we have also shown, these constructions can be extended to scenarios with additional twisted or untwisted fields, and we have also discussed how Starobinsky-like inflationary models can be constructed in this framework.

The models described in this chapter provide a general framework that is suitable for constructing unified supergravity cosmological models that include a primordial near-dS inflationary epoch that is consistent with CMB measurements, the transition to a low-energy effective theory incorporating soft supersymmetry breaking at some scale below that of inflation, and a small present-day cosmological constant (dark energy). As such, this framework is suitable for constructing complete models of cosmology and particle physics below the Planck scale.

4. SUMMARY AND CONCLUSIONS

We constructed Lagrangians and showed new Minkowski and de Sitter solutions with a presence of multiple chiral fields in a framework of 4d $\mathcal{N} = 1$ no-scale supergravity in a unified way. As noted in the Introduction, it is currently debated whether string theory admits de Sitter solutions [14]. If this were not the case, measurements of the accelerating expansion of the Universe [1] and the continuing success of cosmological inflation [2] would suggest that our Universe lies in the swampland. Our working hypothesis is that this is not the case, and that deeper understanding of string theory will reveal how it can accommodate de Sitter solutions. Since no-scale supergravity is the appropriate framework for discussing cosmology at scales hierarchically smaller than the string scale, assuming also that $\mathcal{N} = 1$ supersymmetry holds down to energies $\ll m_{\rm Planck}$, the explorations in this dissertation may provide a helpful guide to the structure of the low-energy effective field theories of de Sitter string solutions. As such, they may even provide some useful signposts towards the construction of such solutions.

For the future, two general classes of issues stand out. One is the construction of specific models for sub-Planckian physics, which should address the incorporation of Standard Model (and possibly other) matter and Higgs degrees of freedom. Should these be described by twisted or untwisted fields, and how are they coupled to the inflaton? Specific answers to some of these issues have been proposed in [53], and more details are forthcoming [54].

Another set of issues concerns the interface with string theory. For example, although no-scale supergravity theories arise generically in the low-energy limits of string compactifications, many different non-compact coset manifolds may be realized. Which of these is to be preferred? Another set of questions concerns the specific forms of superpotential that are needed to obtain a Minkowski or dS vacuum. In papers [12, 13], we have constructed them from a bottom-up approach, and demonstrated their uniqueness. How could one hope to obtain them in a top-down approach, starting from a specific string model?

This question is particularly acute in the case of dS vacuum solutions, since swampland conjec-

tures [4] suggest that string theory may not possess such vacua. At the time of writing controversy still swirls about these conjectures, and in this work we have taken the pragmatic approach of exploring what such solutions would look like. As such, our solutions may suggest avenues to explore in searching for them, or at least the obstacles to be overcome. The existence or otherwise of dS vacua in string theory is clearly a key issue for the future exploration.

Further research extending the Minkowski and de Sitter constructions given in this thesis can be found in [40, 55, 56, 57].

REFERENCES

[1] A. G. Riess *et al.* [Supernova Search Team], Astron. J. **116** (1998) 1009 doi:10.1086/300499 [astro-ph/9805201]; Astrophys. J. **517** (1999) 565 doi:10.1086/307221 [astro-ph/9812133]. For the most recent observational constraints, see N. Aghanim *et al.* [Planck Collaboration], arXiv:1807.06209 [astro-ph.CO].

[2] K. A. Olive, Phys. Rept. **190** (1990) 307; A. D. Linde, *Particle Physics and Inflationary Cosmology* (Harwood, Chur, Switzerland, 1990); D. H. Lyth and A. Riotto, *Phys. Rep.* **314** (1999) 1 [arXiv:hep-ph/9807278]; J. Martin, C. Ringeval and V. Vennin, Phys. Dark Univ. **5-6**, 75-235 (2014) [arXiv:1303.3787 [astro-ph.CO]]; J. Martin, C. Ringeval, R. Trotta and V. Vennin, JCAP **1403** (2014) 039 [arXiv:1312.3529 [astro-ph.CO]]; J. Martin, Astrophys. Space Sci. Proc. **45**, 41 (2016) [arXiv:1502.05733 [astro-ph.CO]]. For the most recent observational constraints, see Y. Akrami *et al.* [Planck Collaboration], arXiv:1807.06211 [astro-ph.CO].

[3] S. Kachru, R. Kallosh, A. D. Linde and S. P. Trivedi, Phys. Rev. D **68**, 046005 (2003) doi:10.1103/PhysRevD.68.046005 [arXiv:hep-th/0301240 [hep-th]].

[4] G. Obied, H. Ooguri, L. Spodyneiko and C. Vafa, [arXiv:1806.08362 [hep-th]].

[5] U. H. Danielsson and T. Van Riet, Int. J. Mod. Phys. D **27**, no.12, 1830007 (2018) doi:10.1142/S0218271818300070 [arXiv:1804.01120 [hep-th]].

[6] E. Cremmer, S. Ferrara, C. Kounnas and D. V. Nanopoulos, Phys. Lett. B **133** (1983) 61;

[7] J. R. Ellis, A. B. Lahanas, D. V. Nanopoulos and K. Tamvakis, Phys. Lett. B **134** (1984) 429.

[8] J. R. Ellis, C. Kounnas and D. V. Nanopoulos, Nucl. Phys. B **241**, 406 (1984). [EKN]

[9] J. R. Ellis, C. Kounnas and D. V. Nanopoulos, Nucl. Phys. B **247**, 373 (1984).

[10] A. B. Lahanas and D. V. Nanopoulos, Phys. Rept. **145** (1987) 1.

[11] E. Witten, Phys. Lett. B **155** (1985) 151.

[12] J. Ellis, B. Nagaraj, D. V. Nanopoulos and K. A. Olive, JHEP **1811** (2018) 110 [arXiv:1809.10114 [hep-th]].

[13] J. Ellis, B. Nagaraj, D. V. Nanopoulos, K. A. Olive and S. Verner, JHEP **10**, 161 (2019) doi:10.1007/JHEP10(2019)161 [arXiv:1907.09123 [hep-th]].

[14] D. G. Boulware and S. Deser, Phys. Lett. B **175**, 409 (1986); S. Kalara and K. A. Olive, Phys. Lett. B **218**, 148 (1989); S. Kalara, C. Kounnas and K. A. Olive, Phys. Lett. B **215**, 265 (1988); S. Kachru, R. Kallosh, A. D. Linde and S. P. Trivedi, Phys. Rev. D **68** (2003) 046005 [hep-th/0301240]; B. Michel, E. Mintun, J. Polchinski, A. Puhm and P. Saad, JHEP **1509** (2015) 021 doi:10.1007/JHEP09(2015)021 [arXiv:1412.5702 [hep-th]]; J. Polchinski, arXiv:1509.05710 [hep-th]; U. H. Danielsson and T. Van Riet, arXiv:1804.01120 [hep-th]; G. Obied, H. Ooguri, L. Spodyneiko and C. Vafa, arXiv:1806.08362 [hep-th]; J. P. Conlon, arXiv:1808.05040 [hep-th]; R. Kallosh and T. Wrase, arXiv:1808.09427 [hep-th]; R. Kallosh, A. Linde, E. McDonough and M. Scalisi, arXiv:1808.09428 [hep-th]; Y. Akrami, R. Kallosh, A. Linde and V. Vardanyan, arXiv:1808.09440 [hep-th]; S. Kachru and S. P. Trivedi, arXiv:1808.08971 [hep-th].

[15] M. Gomez-Reino and C. A. Scrucca, JHEP **0605**, 015 (2006) [hep-th/0602246]; L. Covi, M. Gomez-Reino, C. Gross, J. Louis, G. A. Palma and C. A. Scrucca, JHEP **0806**, 057 (2008) [arXiv:0804.1073 [hep-th]]; L. Covi, M. Gomez-Reino, C. Gross, G. A. Palma and C. A. Scrucca, JHEP **0903**, 146 (2009) [arXiv:0812.3864 [hep-th]]; C. Kounnas, D. Lüst and N. Toumbas, Fortsch. Phys. **63**, 12 (2015) [arXiv:1409.7076 [hep-th]]; M. C. D. Marsh, B. Vercnocke and T. Wrase, JHEP **1505**, 081 (2015) [arXiv:1411.6625 [hep-th]]; D. Gallego, M. C. D. Marsh, B. Vercnocke and T. Wrase, JHEP **1710**, 193 (2017) [arXiv:1707.01095 [hep-th]].

[16] D. Roest and M. Scalisi, Phys. Rev. D **92**, 043525 (2015) [arXiv:1503.07909 [hep-th]].

[17] J. Ellis, D. V. Nanopoulos and K. A. Olive, JCAP **1310**, 009 (2013) [arXiv:1307.3537 [hep-th]].

[18] R. Kallosh, A. Linde and D. Roest, JHEP **1311** (2013) 198 doi:10.1007/JHEP11(2013)198 [arXiv:1311.0472 [hep-th]]; R. Kallosh, A. Linde and D. Roest, JHEP **1408**, 052 (2014) [arXiv:1405.3646 [hep-th]].

[19] J. Ellis, D. V. Nanopoulos and K. A. Olive, Phys. Rev. D **97**, no. 4, 043530 (2018) [arXiv:1711.11051 [hep-th]].

[20] J. R. Ellis, C. Kounnas and D. V. Nanopoulos, Phys. Lett. B **143**, 410 (1984).

[21] R. Kallosh, A. Linde, B. Vercnocke and T. Wrase, JHEP **1410**, 011 (2014) doi:10.1007/JHEP10(2014)011 [arXiv:1406.4866 [hep-th]].

[22] M. Tanabashi *et al.* [Particle Data Group], Phys. Rev. D **98** (2018) no.3, 030001. doi:10.1103/PhysRevD.98.030001

[23] K. A. Olive, Phys. Rept. **190** (1990) 307; A. D. Linde, *Particle Physics and Inflationary Cosmology* (Harwood, Chur, Switzerland, 1990); D. H. Lyth and A. Riotto, *Phys. Rep.* **314** (1999) 1 [arXiv:hep-ph/9807278]; J. Martin, C. Ringeval and V. Vennin, Phys. Dark Univ. **5-6**, 75-235 (2014) [arXiv:1303.3787 [astro-ph.CO]]; J. Martin, C. Ringeval, R. Trotta and V. Vennin, JCAP **1403** (2014) 039 [arXiv:1312.3529 [astro-ph.CO]]; J. Martin, Astrophys. Space Sci. Proc. **45**, 41 (2016) [arXiv:1502.05733 [astro-ph.CO]].

[24] H. P. Nilles, Phys. Rept. **110** (1984) 1.

[25] H. E. Haber and G. L. Kane, Phys. Rept. **117** (1985) 75.

[26] J. R. Ellis, D. V. Nanopoulos, K. A. Olive and K. Tamvakis, Phys. Lett. B **118** (1982) 335.

[27] E. J. Copeland, A. R. Liddle, D. H. Lyth, E. D. Stewart and D. Wands, Phys. Rev. D **49**, 6410 (1994) [astro-ph/9401011]; E. D. Stewart, Phys. Rev. D **51**, 6847 (1995) [hep-ph/9405389]; Also see, for example: A. D. Linde, *Particle Physics and Inflationary Cosmology* (Harwood, Chur, Switzerland, 1990); D. H. Lyth and A. Riotto, *Phys. Rep.* **314** (1999) 1 [arXiv:hep-ph/9807278]. J. Martin, C. Ringeval and V. Vennin, arXiv:1303.3787 [astro-ph.CO].

[28] S. Ferrara and R. Kallosh, Phys. Rev. D **94** (2016) no.12, 126015 doi:10.1103/PhysRevD.94.126015 [arXiv:1610.04163 [hep-th]].

[29] N. Aghanim *et al.* [Planck Collaboration], arXiv:1807.06209 [astro-ph.CO]; Y. Akrami *et al.* [Planck Collaboration], arXiv:1807.06211 [astro-ph.CO].

[30] P. A. R. Ade *et al.* [BICEP2 and Keck Array Collaborations], Phys. Rev. Lett. **121**, 221301 (2018) [arXiv:1810.05216 [astro-ph.CO]].

[31] A. A. Starobinsky, Phys. Lett. B **91**, 99 (1980).

[32] J. Ellis, D. V. Nanopoulos and K. A. Olive, Phys. Rev. Lett. **111** (2013) 111301 [arXiv:1305.1247 [hep-th]].

[33] A. S. Goncharov and A. D. Linde, Class. Quant. Grav. **1**, L75 (1984).

[34] C. Kounnas and M. Quiros, Phys. Lett. B **151**, 189 (1985).

[35] J. R. Ellis, K. Enqvist, D. V. Nanopoulos, K. A. Olive and M. Srednicki, Phys. Lett. **152B** (1985) 175 Erratum: [Phys. Lett. **156B** (1985) 452].

[36] K. Enqvist, D. V. Nanopoulos and M. Quiros, Phys. Lett. B **159**, 249 (1985); P. Binétruy and M. K. Gaillard, Phys. Rev. D **34**, 3069 (1986); H. Murayama, H. Suzuki, T. Yanagida and J. Yokoyama, Phys. Rev. D **50**, 2356 (1994) [arXiv:hep-ph/9311326]; S. C. Davis and M. Postma, JCAP **0803**, 015 (2008) [arXiv:0801.4696 [hep-ph]]; S. Antusch, M. Bastero-Gil, K. Dutta, S. F. King and P. M. Kostka, JCAP **0901**, 040 (2009) [arXiv:0808.2425 [hep-ph]]; S. Antusch, M. Bastero-Gil, K. Dutta, S. F. King and P. M. Kostka, Phys. Lett. B **679**,

428 (2009) [arXiv:0905.0905 [hep-th]]; R. Kallosh and A. Linde, JCAP **1011**, 011 (2010) [arXiv:1008.3375 [hep-th]]; R. Kallosh, A. Linde and T. Rube, Phys. Rev. D **83**, 043507 (2011) [arXiv:1011.5945 [hep-th]]; S. Antusch, K. Dutta, J. Erdmenger and S. Halter, JHEP **1104** (2011) 065 [arXiv:1102.0093 [hep-th]]; R. Kallosh, A. Linde, K. A. Olive and T. Rube, Phys. Rev. D **84**, 083519 (2011) [arXiv:1106.6025 [hep-th]]; T. Li, Z. Li and D. V. Nanopoulos, JCAP **1402**, 028 (2014) [arXiv:1311.6770 [hep-ph]]; W. Buchmuller, C. Wieck and M. W. Winkler, Phys. Lett. B **736**, 237 (2014) [arXiv:1404.2275 [hep-th]].

[37] J. Ellis, D. V. Nanopoulos and K. A. Olive, JCAP **1310** (2013) 009 [arXiv:1307.3537 [hep-th]].

[38] J. Ellis, D. V. Nanopoulos, K. A. Olive and S. Verner, JHEP **1903** (2019) 099 [arXiv:1812.02192 [hep-th]].

[39] J. Ellis, D. V. Nanopoulos, K. A. Olive and S. Verner, arXiv:1903.05267 [hep-ph].

[40] J. Ellis, D. V. Nanopoulos, K. A. Olive and S. Verner, arXiv:1906.10176 [hep-th].

[41] M. C. Romao and S. F. King, JHEP **1707**, 033 (2017) [arXiv:1703.08333 [hep-ph]]; S. F. King and E. Perdomo, JHEP **1905**, 211 (2019) [arXiv:1903.08448 [hep-ph]].

[42] R. Kallosh and A. Linde, JCAP **1306**, 028 (2013) [arXiv:1306.3214 [hep-th]].

[43] F. Farakos, A. Kehagias and A. Riotto, Nucl. Phys. B **876**, 187 (2013) [arXiv:1307.1137 [hep-th]].

[44] S. Ferrara, A. Kehagias and A. Riotto, Fortsch. Phys. **62**, 573 (2014) [arXiv:1403.5531 [hep-th]]; S. Ferrara, A. Kehagias and A. Riotto, Fortsch. Phys. **63**, 2 (2015) [arXiv:1405.2353 [hep-th]]; R. Kallosh, A. Linde, B. Vercnocke and W. Chemissany, JCAP **1407**, 053 (2014) [arXiv:1403.7189 [hep-th]]; K. Hamaguchi, T. Moroi and T. Terada, Phys. Lett. B **733**, 305 (2014) [arXiv:1403.7521 [hep-ph]]; J. Ellis, M. A. G. García, D. V. Nanopoulos and

K. A. Olive, JCAP **1405**, 037 (2014) [arXiv:1403.7518 [hep-ph]]; J. Ellis, M. A. G. García, D. V. Nanopoulos and K. A. Olive, JCAP **1408**, 044 (2014) [arXiv:1405.0271 [hep-ph]].

[45] T. Li, Z. Li and D. V. Nanopoulos, JCAP **1404**, 018 (2014) [arXiv:1310.3331 [hep-ph]]; J. Ellis, D. V. Nanopoulos and K. A. Olive, Phys. Rev. D **89** (2014) 4, 043502 [arXiv:1310.4770 [hep-ph]]; C. P. Burgess, M. Cicoli and F. Quevedo, JCAP **1311** (2013) 003 [arXiv:1306.3512 [hep-th]]; S. Ferrara, R. Kallosh, A. Linde and M. Porrati, Phys. Rev. D **88** (2013) 8, 085038 [arXiv:1307.7696 [hep-th]]; W. Buchmüller, V. Domcke and C. Wieck, Phys. Lett. B **730**, 155 (2014) [arXiv:1309.3122 [hep-th]]; C. Pallis, JCAP **1404**, 024 (2014) [arXiv:1312.3623 [hep-ph]]; C. Pallis, JCAP **1408**, 057 (2014) [arXiv:1403.5486 [hep-ph]]; I. Antoniadis, E. Dudas, S. Ferrara and A. Sagnotti, Phys. Lett. B **733**, 32 (2014) [arXiv:1403.3269 [hep-th]]; T. Li, Z. Li and D. V. Nanopoulos, Eur. Phys. J. C **75**, no. 2, 55 (2015) [arXiv:1405.0197 [hep-th]]; W. Buchmuller, E. Dudas, L. Heurtier and C. Wieck, JHEP **1409**, 053 (2014) [arXiv:1407.0253 [hep-th]]; J. Ellis, M. A. G. García, D. V. Nanopoulos and K. A. Olive, JCAP **1501**, no. 01, 010 (2015) [arXiv:1409.8197 [hep-ph]]; T. Terada, Y. Watanabe, Y. Yamada and J. Yokoyama, JHEP **1502**, 105 (2015) [arXiv:1411.6746 [hep-ph]]; W. Buchmuller, E. Dudas, L. Heurtier, A. Westphal, C. Wieck and M. W. Winkler, JHEP **1504**, 058 (2015) [arXiv:1501.05812 [hep-th]]; A. B. Lahanas and K. Tamvakis, Phys. Rev. D **91**, no. 8, 085001 (2015) [arXiv:1501.06547 [hep-th]].

[46] J. Ellis, M. A. G. García, D. V. Nanopoulos and K. A. Olive, JCAP **1510**, 003 (2015) [arXiv:1503.08867 [hep-ph]].

[47] J. Ellis, M. A. G. García, D. V. Nanopoulos and K. A. Olive, JCAP **1507**, no. 07, 050 (2015) [arXiv:1505.06986 [hep-ph]];

[48] I. Dalianis and F. Farakos, JCAP **1507**, no. 07, 044 (2015) [arXiv:1502.01246 [gr-qc]]. I. Garg and S. Mohanty, Phys. Lett. B **751**, 7 (2015) [arXiv:1504.07725 [hep-ph]]; E. Dudas and C. Wieck, JHEP **1510**, 062 (2015) [arXiv:1506.01253 [hep-th]]; M. Scalisi, JHEP **1512**, 134 (2015) [arXiv:1506.01368 [hep-th]]; S. Ferrara, A. Kehagias and M. Porrati, JHEP **1508**,

001 (2015) [arXiv:1506.01566 [hep-th]]; J. Ellis, M. A. G. García, D. V. Nanopoulos and K. A. Olive, Class. Quant. Grav. **33**, no. 9, 094001 (2016) [arXiv:1507.02308 [hep-ph]]; A. Addazi and M. Y. Khlopov, Phys. Lett. B **766**, 17 (2017) [arXiv:1612.06417 [gr-qc]]; C. Pallis and N. Toumbas, Adv. High Energy Phys. **2017**, 6759267 (2017) [arXiv:1612.09202 [hep-ph]]; T. Kobayashi, O. Seto and T. H. Tatsuishi, PTEP **2017**, no. 12, 123B04 (2017) [arXiv:1703.09960 [hep-th]]; E. Dudas, T. Gherghetta, Y. Mambrini and K. A. Olive, Phys. Rev. D **96**, no. 11, 115032 (2017) [arXiv:1710.07341 [hep-ph]]; I. Garg and S. Mohanty, Int. J. Mod. Phys. A **33**, no. 21, 1850127 (2018) [arXiv:1711.01979 [hep-ph]]; W. Ahmed and A. Karozas, Phys. Rev. D **98**, no. 2, 023538 (2018) [arXiv:1804.04822 [hep-ph]]. Y. Cai, R. Deen, B. A. Ovrut and A. Purves, JHEP **1809**, 001 (2018) [arXiv:1804.07848 [hep-th]]. S. Khalil, A. Moursy, A. K. Saha and A. Sil, Phys. Rev. D **99**, no. 9, 095022 (2019) [arXiv:1810.06408 [hep-ph]].

[49] J. Ellis, M. A. G. García, N. Nagata, D. V. Nanopoulos and K. A. Olive, JCAP **1611**, no. 11, 018 (2016) [arXiv:1609.05849 [hep-ph]].

[50] J. Ellis, M. A. G. García, N. Nagata, D. V. Nanopoulos and K. A. Olive, JCAP **1707**, no. 07, 006 (2017) [arXiv:1704.07331 [hep-ph]]; J. Ellis, M. A. G. García, N. Nagata, D. V. Nanopoulos and K. A. Olive, JCAP **1904**, no. 04, 009 (2019) [arXiv:1812.08184 [hep-ph]].

[51] R. Kallosh, A. Linde and D. Roest, JHEP **1311**, 198 (2013). [arXiv:1311.0472 [hep-th]].

[52] A. Linde, JCAP **1505**, 003 (2015). [arXiv:1504.00663 [hep-th]].

[53] J. Ellis, M. A. G. Garcia, N. Nagata, D. V. Nanopoulos and K. A. Olive, arXiv:1906.08483 [hep-ph].

[54] J. Ellis, M. A. G. Garcia, N. Nagata, D. V. Nanopoulos and K. A. Olive, *in preparation*.

[55] J. Ellis, D. V. Nanopoulos, K. A. Olive and S. Verner, JCAP **08**, 037 (2020) doi:10.1088/1475-7516/2020/08/037 [arXiv:2004.00643 [hep-ph]].

[56] I. Antoniadis, D. V. Nanopoulos and J. Rizos, JCAP **03**, 017 (2021) doi:10.1088/1475-7516/2021/03/017 [arXiv:2011.09396 [hep-th]].

[57] I. Antoniadis, D. V. Nanopoulos and J. Rizos, Eur. Phys. J. C **82**, no.4, 377 (2022) doi:10.1140/epjc/s10052-022-10353-6 [arXiv:2112.01211 [hep-th]].

APPENDIX A

SUPERPOTENTIALS WITH INTEGER POWERS

A.1 1-Field Model

Superpotential for Minkowski solution in 1-field model is of the form

$$W = \phi^{n_\pm}, \tag{A.1}$$

where

$$n_\pm = \frac{3}{2}(\alpha \pm \sqrt{\alpha}). \tag{A.2}$$

From the above equation, it is clear that integer powers can be gotten by just choosing an appropriate α.

On the other hand, superpotential for de Sitter solution is of the form

$$W = \phi^{n_+} - \phi^{n_-}. \tag{A.3}$$

To have integer powers, we need $3\alpha = n_+ + n_-$ and $3\sqrt{\alpha} = n_+ - n_-$ to be integers. Thus the powers satisfy

$$(n_+ - n_-)^2 = 3(n_+ + n_-). \tag{A.4}$$

From the above equations, it is easy to get the following pair of integer powers and α s:

$$\begin{gathered}(n_-, n_+) = \{(0,3), (3,9), (9,18), (18,30), (30,45), (45,63), (63,84), ...\} \\ \alpha = \{\ 1\ ,\ 4\ ,\ 9\ ,\ 16\ ,\ 25\ ,\ 36\ ,\ 49\ , ...\}\end{gathered} \tag{A.5}$$

The pattern is pretty clear: n_- of a pair is always the n_+ of the previous pair and the difference $n_+ - n_-$ is multiple of 3. The α s are just squares of natural numbers. Since $\alpha \geq 1$ for each of the

integer solutions, all the dS solutions are also stable. In Fig. (A.1), we plot all the integer power solutions.

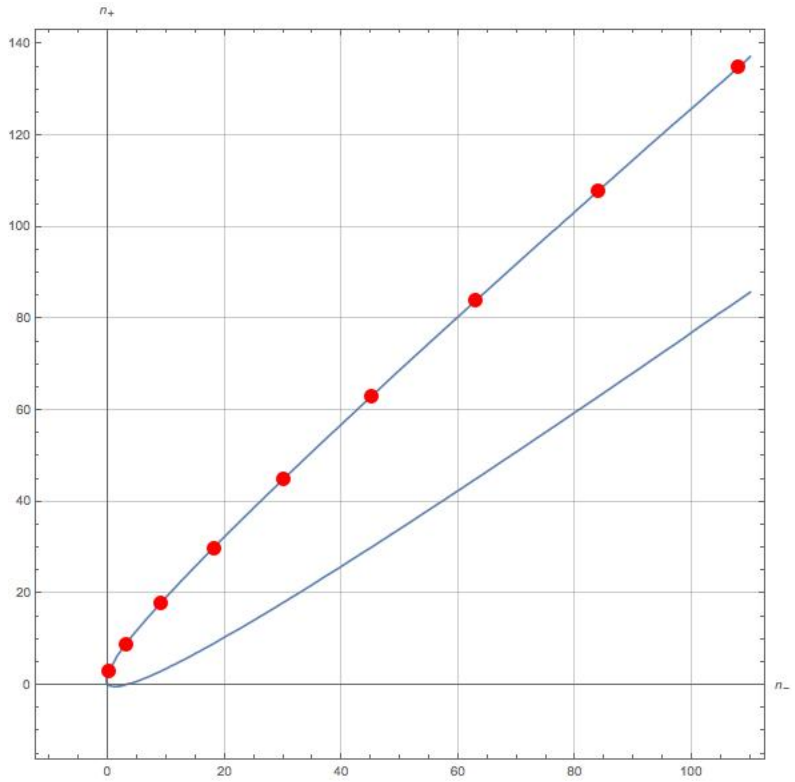

Figure A.1: The curve is $(n_+ - n_-)^2 = 3(n_+ + n_-)$. The red dots correspond to points where both n_- and n_+ are integers and $n_+ > n_-$.

A.2 2-Field Model

De Sitter solutions: Let (n_{1+}, n_{2+}) and (n_{1-}, n_{2-}) be two antipodal points such that their co-ordinates are integers. Then the mid-point of these antipodal points give the center of the ellipse on which they lie. This implies

$$\begin{aligned} 3\alpha_1 &= n_{1+} + n_{1-}, \\ 3\alpha_2 &= n_{2+} + n_{2-}. \end{aligned} \tag{A.6}$$

Now using the fact that each of the points (n_{1+}, n_{2+}) and (n_{1-}, n_{2-}) lie on the ellipse we get the following equation:

$$\frac{(n_{1+} - n_{1-})^2}{n_{1+} + n_{1-}} + \frac{(n_{2+} - n_{2-})^2}{n_{2+} + n_{2-}} = 3. \tag{A.7}$$

Notice that both the terms on the LHS are non-negative numbers. Also notice that the first term is made up of only n_{1+}, n_{1-} and the second term is made up of only n_{2+}, n_{2-}. Therefore, the only way the above equation can hold is if each term is a constant adding up to 3:

$$\frac{(n_{1+} - n_{1-})^2}{n_{1+} + n_{1-}} = \lambda_1, \qquad \frac{(n_{2+} - n_{2-})^2}{n_{2+} + n_{2-}} = \lambda_2, \tag{A.8}$$

with conditions $0 \leq \lambda_1 \leq 3$, $0 \leq \lambda_2 \leq 3$ and $\lambda_1 + \lambda_2 = 3$. Let us rewrite the above equations so that they look like Eq. (A.4) that we got for 1-field model.

$$(n_{1+} - n_{1-})^2 = \lambda_1(n_{1+} + n_{1-}), \tag{A.9}$$

$$(n_{2+} - n_{2-})^2 = \lambda_2(n_{2+} + n_{2-}). \tag{A.10}$$

Now it is easy to get integer solutions. We will work out two cases to illustrate the procedure.

Case 1:

Let us choose $\lambda_1 = 3$ and $\lambda_2 = 0$. Then Eq. (A.9) and Eq. (A.10) are

$$(n_{1+} - n_{1-})^2 = 3(n_{1+} + n_{1-}), \tag{A.11}$$

$$n_{2+} = n_{2-}. \tag{A.12}$$

We already solved Eq. (A.11) when we were doing 1-field model. Therefore, we know all the solutions:

$$\begin{aligned}\{(n_{1-}, n_{2-}), (n_{1+}, n_{2+})\} = \{&(0, n_{2-}), (3, n_{2-}),\\ &(3, n_{2-}), (9, n_{2-}),\\ &(9, n_{2-}), (18, n_{2-}),\\ &(18, n_{2-}), (30, n_{2-}),\\ &(30, n_{2-}), (45, n_{2-}),\\ &(45, n_{2-}), (63, n_{2-}),\\ &....\}\end{aligned} \tag{A.13}$$

In the above sequence n_{2-} could be any non-negative integer. From the above solutions, we can easily find out α_1 and α_2 using Eq. (A.6).

Case 2:

Let us work with a little non-trivial values for λ_1 and λ_2. Let

$$\lambda_1 = 1.2, \qquad \lambda_2 = 2.8. \tag{A.14}$$

Therefore, we need to solve for

$$(n_{1+} - n_{1-})^2 = 1.2(n_{1+} + n_{1-}), \tag{A.15}$$

$$(n_{2+} - n_{2-})^2 = 2.8(n_{2+} + n_{2-}). \tag{A.16}$$

The solutions to the equations are plotted in Fig. (A.2) and Fig. (A.3). The integer solutions for Eq. (A.15) are:

$$\{(n_{1-}, n_{1+})\} = \{(0, 0), (12, 18), (18, 12), (54, 66), (66, 54), ...\}. \tag{A.17}$$

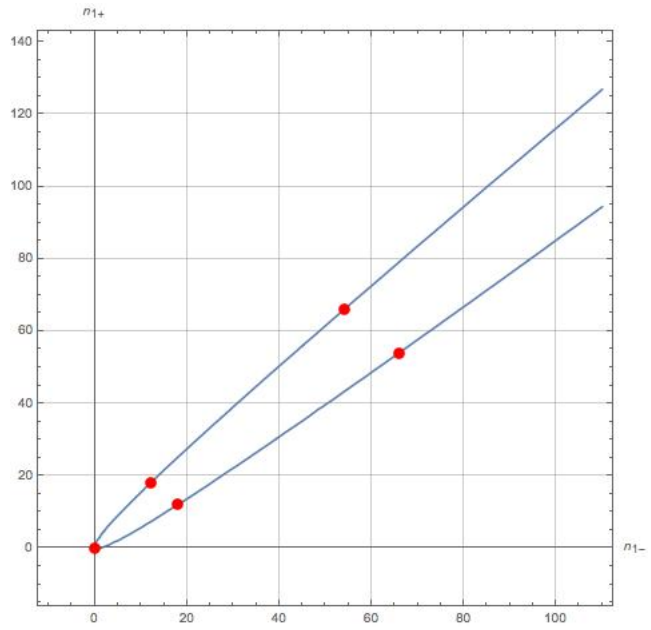

Figure A.2: The curve is $(n_{1+} - n_{1-})^2 = 1.2(n_{1+} + n_{1-})$. The red dots correspond to points where both n_{1+} and n_{1-} are integers.

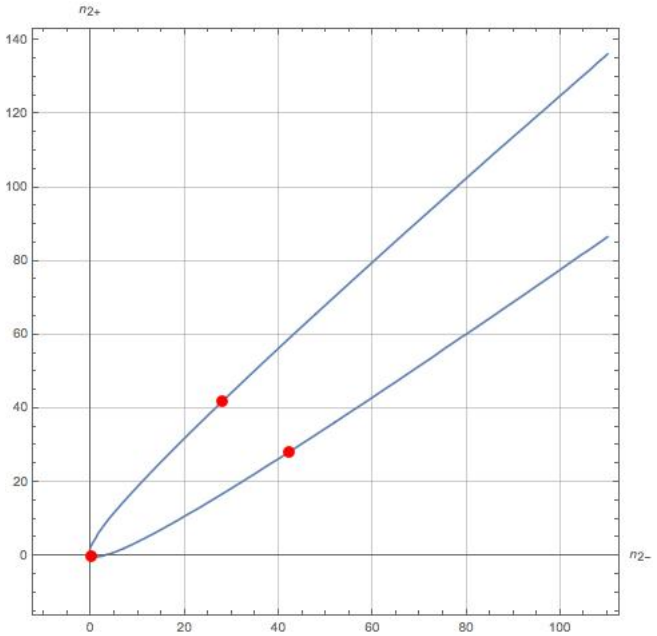

Figure A.3: The curve is $(n_{2+} - n_{2-})^2 = 2.8(n_{2+} + n_{2-})$. The red dots correspond to points where both n_{2+} and n_{2-} are integers.

The integer solutions for Eq. (A.16) are:

$$\{(n_{2-}, n_{2+})\} = \{(0,0), (28,42), (42,28), ...\}. \tag{A.18}$$

Now we can combine one of the solutions in Eq. (A.17) and Eq. (A.18) to construct antipodal points both of which are non-negative integers. For example, we can take $(n_{1-}, n_{1+}) = (12, 18)$ and $(n_{2-}, n_{2+}) = (28, 42)$. This would give us $(n_{1+}, n_{2+}) = (18, 42)$ and $(n_{1-}, n_{2-}) = (12, 28)$ as antipodal points. α_1 and α_2 can be found using Eq. (A.6). This gives us

$$\alpha_1 = \frac{n_{1+} + n_{1-}}{3} = \frac{18 + 12}{3} = 10, \tag{A.19}$$

$$\alpha_2 = \frac{n_{2+} + n_{2-}}{3} = \frac{42 + 28}{3} = \frac{70}{3}. \tag{A.20}$$

APPENDIX B

STABILITY ANALYSIS OF TWO-FIELD dS SOLUTIONS

B.1 Stability Analysis

As in the single-field case, the de Sitter solutions of the two-field model are not stable. However, stable solutions can easily be found by deforming the Kähler potential to include a stabilizing quartic term:

$$K \;=\; -\,3\sum_{i=1}^{2}\alpha_i \ln(\phi_i+\phi_i^\dagger+b_i(\phi_i-\phi_i^\dagger)^4)\,. \tag{B.1}$$

With this modification the potential along real field directions is still given by Eq. (2.36). To prove the stability of the two-field de Sitter solution with the quartic modification of the Kähler potential, we calculate the Hessian matrix $\partial^2 V/\partial y_i \partial y_j : i,j=1,2$ along the real field directions, and demand that it be positive semi-definite. The Hessian matrix along the real field directions is of the form

$$a^2\left(\frac{3.2^{1-3\alpha_1-3\alpha_2}}{\alpha_2 r_1^2+\alpha_1 r_2^2}\right)\begin{bmatrix} x_1^{-2}A_1 & x_1^{-1}x_2^{-1}B \\ x_1^{-1}x_2^{-1}B & x_2^{-2}A_2 \end{bmatrix}\,, \tag{B.2}$$

where

$$A_1 = w^{-1}\left(\alpha_1^2 r_2^2(1+4w+w^2)+\alpha_1\alpha_2 r_1^2(1-w)^2+\alpha_2 r_1^2(96b_1x_1^3-1)(1+w)^2\right), \tag{B.3}$$

$$A_2 = w^{-1}\left(\alpha_2^2 r_1^2(1+4w+w^2)+\alpha_1\alpha_2 r_2^2(1-w)^2+\alpha_1 r_2^2(96b_2x_2^3-1)(1+w)^2\right), \tag{B.4}$$

$$B = -6\alpha_1\alpha_2 r_1 r_2 \tag{B.5}$$

and defined

$$w \equiv x_1^{\frac{3r_1}{\sqrt{\frac{r_1^2}{\alpha_1}+\frac{r_2^2}{\alpha_2}}}}\, x_2^{\frac{3r_2}{\sqrt{\frac{r_1^2}{\alpha_1}+\frac{r_2^2}{\alpha_2}}}}. \tag{B.6}$$

The condition for the Hessian matrix to be positive semi-definite can be worked out to be

$$A_1 A_2 \geq B^2 \,. \tag{B.7}$$

In order to analyze the stability of de Sitter solutions, let us start with a very simplified version of inequality (B.7) by having $\alpha_1 = \alpha_2 = \alpha$ and $\vec{r} = (1/\sqrt{2}, 1/\sqrt{2})$. Then the condition given by Eq. (B.7) is just

$$\begin{aligned} &\left(2\alpha(1+w+w^2) + (96 b_1 x_1^3 - 1)(1+w)^2\right) \\ &\times \left(2\alpha(1+w+w^2) + (96 b_2 x_2^3 - 1)(1+w)^2\right) \;\geq\; 36\alpha^2 w^2 \,. \end{aligned} \tag{B.8}$$

Our strategy will be to treat w as a parameter and eliminate x_2 in favour of x_1 via Eq. (B.6). Then inequality Eq. (B.8) is just

$$\begin{aligned} &\left(2\alpha(1+w+w^2) + (96 b_1 x_1^3 - 1)(1+w)^2\right) \\ &\times \left(2\alpha(1+w+w^2) + \left(96 b_2 \frac{w^{\sqrt{2/\alpha}}}{x_1^3} - 1\right)(1+w)^2\right) - 36\alpha^2 w^2 \;\geq\; 0 \,. \end{aligned} \tag{B.9}$$

Notice that for $x_1 \gg 1$, $(96 b_1 x_1^3 - 1)$ dominates and for $x_1 \ll 1$, $\left(96 b_2 \frac{w^{\sqrt{2/\alpha}}}{x_1^3} - 1\right)$ dominates. Therefore, near $x_1 \approx 1$, the LHS of Eq. (B.9) has an extremum. Differentiating the LHS of Eq. (B.9) once with respect to x_1, we get

$$288 x_1^{-4}(1+w)^2\left(2\alpha(1+w+w^2) - (1+w)^2\right)\left(b_1 x_1^6 - b_2 w^{\sqrt{2/\alpha}}\right) \tag{B.10}$$

It is clear that the extremum occurs at $x_1 = (b_2/b_1)^{1/6}\, w^{1/(3\sqrt{2\alpha})}$ and that it is a global extremum. Whether the extremum is a maximum or a minimum depends on the sign of $2\alpha(1+w+w^2) - (1+w)^2$ and it is non-negative for

$$\alpha \geq \frac{2}{3} \,. \tag{B.11}$$

We certainly don't want the LHS of inequality Eq. (B.9) to have global maximum. Therefore, we need $\alpha \geq 2/3$ if we are to have any hope of satisfying Eq. (B.9). It is not just enough to have a global minimum, but it should also be non-negative. This may impose some constraints on the range of values of b_1 and b_2. It can be checked that with $b_1 = b_2 = 1$ and $\alpha \geq 2/3$, the stability condition Eq. (B.9) is always satisfied irrespective of the value of w.

Now we will use similar strategy to analyze the stability condition for generic α_1, α_2 and $\vec{r}$. We will consider w and $\vec{r}$ as parameters. Then the stability condition Eq. (B.7) in terms of just x_1 is

$$\begin{aligned}
&\left(\alpha_1^2 r_2^2(1+4w+w^2) + \alpha_1\alpha_2 r_1^2(1-w)^2 + \alpha_2 r_1^2(96b_1x_1^3-1)(1+w)^2\right) \\
&\left(\alpha_2^2 r_1^2(1+4w+w^2) + \alpha_1\alpha_2 r_2^2(1-w)^2 + \alpha_1 r_2^2\left(96b_2\frac{w^{\frac{1}{r_2}\sqrt{\frac{r_1^2}{\alpha_1}+\frac{r_2^2}{\alpha_2}}}}{x_1^{(3r_1/r_2)}} - 1\right)(1+w)^2\right) \qquad \text{(B.12)} \\
&- 36\alpha_1^2\alpha_2^2 r_1^2 r_2^2 w^2 \geq 0.
\end{aligned}$$

Case 1: $r_1/r_2 > 0$

When $r_1/r_2 > 0$, $(96b_1x_1^3 - 1)$ term dominates for $x_1 \gg 1$ and, $\left(96b_2\frac{w^{\frac{1}{r_2}\sqrt{\frac{r_1^2}{\alpha_1}+\frac{r_2^2}{\alpha_2}}}}{x_1^{(3r_1/r_2)}} - 1\right)$ dominates for $x_1 \ll 1$. Therefore, near $x_1 \approx 1$, the LHS of Eq. (B.12) has an extremum. Similar to what we did before, we can find the point of extremum and demand the second derivative calculated at that point be non-negative. For simplicity, we will take $b_1 = b_2 = 1$ and $\vec{r} = (1/\sqrt{2}, 1/\sqrt{2})$. Then we get the following two conditions:

$$\alpha_1^2(1+4w+w^2) + \alpha_1\alpha_2(1-w)^2 - \alpha_2(1+w)^2 \geq 0, \qquad \text{(B.13)}$$

$$\alpha_2^2(1+4w+w^2) + \alpha_1\alpha_2(1-w)^2 - \alpha_1(1+w)^2 \geq 0. \qquad \text{(B.14)}$$

To satisfy the above inequalities, we just demand that each quadratic polynomial in w on the LHS

have imaginary roots. This leads to the following inequalities:

$$3\alpha_1^3 - 2\alpha_1\alpha_2 - 6\alpha_1^2\alpha_2 + 4\alpha_2^2 \leq 0, \tag{B.15}$$

$$3\alpha_2^3 - 2\alpha_1\alpha_2 - 6\alpha_1\alpha_2^2 + 4\alpha_1^2 \leq 0. \tag{B.16}$$

We plot the corresponding region in α_1, α_2 space in Fig. (B.1). This is the region where the LHS of Eq. (B.12) (for $\vec{r} = (1/\sqrt{2}, 1/\sqrt{2})$ and $b_1 = b_2 = 1$) has a global minimum. We also need the global minimum to be non-negative. At several points in this region, when checked indeed produced a non-negative minimum for all values of w. As can be seen from the figure, there are three kinks with one being at $(\alpha_1, \alpha_2) = (2/3, 2/3)$.

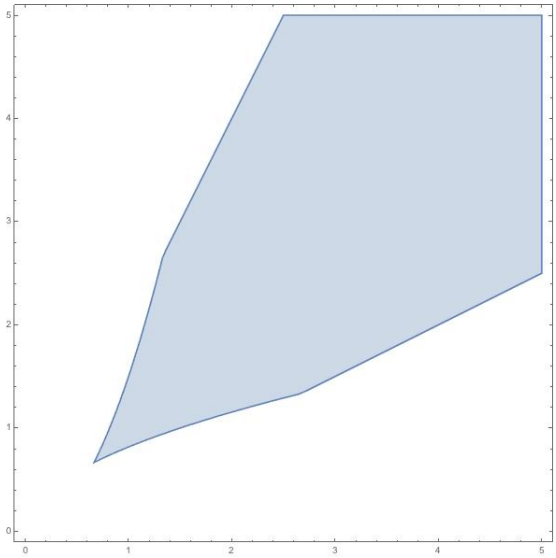

Figure B.1: The region where the LHS of Eq. (B.12) (for $\vec{r} = (1/\sqrt{2}, 1/\sqrt{2})$ and $b_1 = b_2 = 1$) has a global minimum.

Case 2: $r_1/r_2 < 0$

When $r_1/r_2 < 0$, both $(96b_1x_1^3 - 1)$ and $\left(96b_2 \frac{w^{\frac{1}{r_2}\sqrt{\frac{r_1^2}{\alpha_1} + \frac{r_2^2}{\alpha_2}}}}{x_1^{(3r_1/r_2)}} - 1\right)$ terms dominate for $x_1 \gg 1$. Then

we should expect that LHS of Eq. (B.12) has an extremum near $x_1 \approx 0$. For simplicity, we will take $b_1 = b_2 = 1$ and $\vec{r} = (-1/\sqrt{2}, 1/\sqrt{2})$. With this simplification, we indeed get an extremum at $x_1 = 0$. By plugging in $x_1 = 0$ in Eq. (B.12) for our case, it is clear that the stabilization terms disappear. Without stabilization terms, such an inequality cannot be satisfied. Hence the are no stable de Sitter solutions.

Case 3: $r_1/r_2 = 0$

This corresponds to having $\vec{r} = (0, 1)$. For simplicity, let us take $b_1 = b_2 = 1$. Then inequality Eq. (B.12) reduces to

$$\alpha_2(1-w)^2 + (1+w)^2(96w^{1/\sqrt{\alpha_2}} - 1) \geq 0. \tag{B.17}$$

This inequality is always satisfied for $\alpha_2 \geq 1$.

Case 4: $r_2/r_1 = 0$

This corresponds to having $\vec{r} = (1, 0)$. For simplicity, let us take $b_1 = b_2 = 1$. Then this is just like the previous case and the stability condition Eq. (B.7) is just $\alpha_1 \geq 1$.

In summary, we can get stable de Sitter solutions only when $\vec{r}$ is in either first or third quadrant.